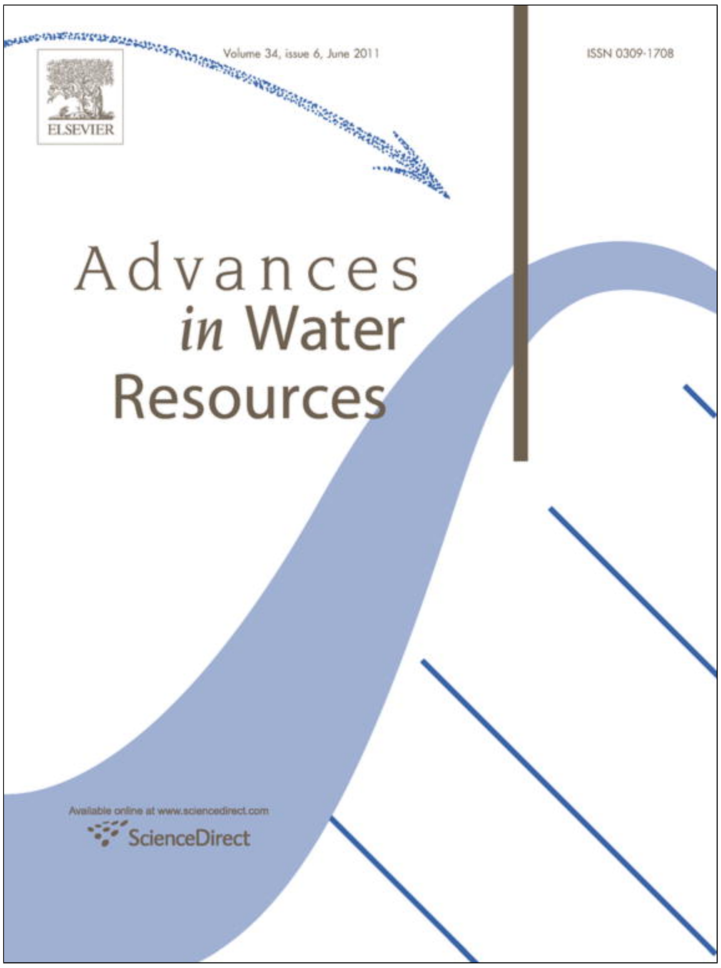
Volume 34, issue 6, June 2011
ISSN 0309-1708
ELSEVIER
Advances
in Water
Resources
Available online at www.sciencedirect.com
ScienceDirect

Advances in Water Resources 34 (2011) 684–700

Contents lists available at ScienceDirect

Advances in Water Resources

journal homepage: www.elsevier.com/locate/advwatres

Global water resources modeling with an integrated model of the social–economic–environmental system

Evan G.R. Davies [a,*], Slobodan P. Simonovic [b,1]

[a] Department of Civil and Environmental Engineering, University of Alberta, Edmonton, Alberta, Canada
[b] Department of Civil and Environmental Engineering, University of Western Ontario, London, Ontario, Canada

ARTICLE INFO

Article history:
Received 9 July 2010
Received in revised form 13 February 2011
Accepted 14 February 2011
Available online 18 February 2011

Keywords:
Climate change
Global change
Integrated assessment
Sustainability
System dynamics
Water resources

ABSTRACT

Awareness of increasing water scarcity has driven efforts to model global water resources for improved insight into water resources infrastructure and management strategies. Most water resources models focus explicitly on water systems and represent socio-economic and environmental change as external drivers. In contrast, the system dynamics-based integrated assessment model employed here, ANEMI, incorporates dynamic representations of these systems, so that their broader changes affect and are affected by water resources systems through feedbacks. Sectors in ANEMI therefore include the global climate system, carbon cycle, economy, population, land use and agriculture, and novel versions of the hydrological cycle, global water use and water quality. Since the model focus is on their interconnections through explicit nonlinear feedbacks, simulations with ANEMI provide insight into the nature and structure of connections between water resources and socio-economic and environmental change. Of particular interest to water resources researchers and modelers will be the simulated effects of a new water stress definition that incorporates both water quality and water quantity effects into the measurement of water scarcity. Five simulation runs demonstrate the value of wastewater treatment and reuse programs and the feedback-effects of irrigated agriculture and greater consumption of animal products.

1. Introduction

Demand for fresh water is rising but a variety of factors including population growth, water pollution, economic progress, land-use change and climate change render its availability into the future uncertain. Awareness of growing water scarcity has led to increasing interest in global modeling of water resources [5], both in terms of supply and demand, with the aim of developing and implementing appropriate water resources infrastructure and management strategies. Such planning requires accurate long-term projections of water supply and demand, but these projections are generally flawed [46] because of inaccuracies in assumptions about, and incomplete understanding of, the driving forces behind domestic, industrial and agricultural water use. Uncertainties surrounding climate change only compound the problem.

Many global water resources models focus exclusively on water-related processes and therefore incorporate socio-economic and broader environmental changes as scenarios, or external drivers. However, interactions between physical processes, biological and biochemical processes, and human-mediated processes are key in determining changes in the global water system [4,109,47]. The main advantage of the approach presented in this paper is therefore the explicit incorporation in an integrated assessment model (IA model) of important hydrological sectors and their socio-economic and natural context. The model, ANEMI [27–29], allows an investigation of the broader feedback-effects of various water resources policies, including those related to wastewater treatment and reuse, and the expansion of irrigated agriculture and changes in the human diet, on the society-biosphere-climate system as a whole. ANEMI provides insight into the behavior of the modeled system: although simulation models can serve as predictive tools, their more important role, as investigated in this and other IA work, relates to learning. They make assumptions about real-world processes and characteristics explicit and therefore offer an opportunity to improve our understanding – and our management – of the modeled system.

The paper begins with an introduction to water resources and integrated assessment, followed by a description of ANEMI. The next section summarizes experimentation undertaken to date and then describes and analyzes three water resources policies through feedback analysis. The paper concludes with a discussion of the role different feedbacks play in determining the simulated behavior of the model and of the implications of the experimental results for real-world water resources management.

* Corresponding author. Tel.: +1 780 492 5134; fax: +1 780 492 0249.
E-mail addresses: evan.davies@ualberta.ca (E.G.R. Davies), simonovic@uwo.ca (S.P. Simonovic).
[1] Tel.: +1 519 661 4075; fax: +1 519 661 3779.

0309-1708/$ - see front matter © 2011 Elsevier Ltd. All rights reserved.
doi:10.1016/j.advwatres.2011.02.010

2. Water resources and integrated assessment

Integrated assessment (IA) focuses on feedbacks between components of a larger system. IA has three aims: (1) to evaluate the broad consequences of and responses to climate and global change, (2) to structure knowledge and characterize uncertainty and (3) to place climate change in the context of other environmental, social and economic changes that might occur over the same time [76]. Rather than answering specific questions, IA provides "insight [into] the nature and structure of the problem, what matters, and what we still need to learn" [76]. Importantly, integrated assessment seeks to inform policy-making [103].

Historically, integrated assessment has focused less on the specific details of component parts of the system and more on their interconnections through feedbacks. As analytical tools, IA models "assemble information that is being created at the various disciplinary frontiers, so as to uncover and quantify implications and feedbacks that might otherwise go unappreciated" in a program of disciplinary research [34, p. 297]. They allow an exploration of the interactions and feedbacks between subsystems, provide flexible and fast simulation tools, structure present knowledge and identify and rank major uncertainties, and supply tools for communication between scientists, the public, and policy makers [88].

In the context of water resources, a variety of model types at river-basin to global scales include hydrologically-relevant variables – global-scale hydrological, vegetation, agricultural, climate and integrated assessment models are discussed first. Global hydrological models are a relatively new development, and result from the same sorts of global change questions that drive integrated assessments. Arnell [10], Vörösmarty et al. [108], Alcamo et al. [5] and Hanasaki et al. [49] produced high-resolution models called, respectively, Macro-PDM, the water balance model (WBM), WaterGAP2 and H08, each of which resolves individual river basins. In addition to hydrological variables, WBM, WaterGAP2 and H08 included both the anthropogenic drivers that change water-use patterns and their quantitative effects on surface water resources. Also at the global scale, Rost et al. [86] developed a dynamic vegetation and water balance model, LPJmL, to simulate the establishment and behavior of natural and agricultural systems and their associated carbon and water fluxes, while Cai and Rosegrant [20] described a basin-scale model, IMPACT-WATER (since updated and called WATERSIM [30], for forecasting domestic, livestock, industrial and irrigation water use and supply in 69 basins to 2025. Siebert and Döll [92] developed a high-resolution model for global agriculture, GCWM, and used it to simulate both irrigated and rain-fed water use under 1998–2002 climatic conditions for 26 different crop classes. However, these models focused exclusively on water resources problems and so used prescribed scenarios for key socio-economic variables – for example, Arnell [12] and Alcamo et al. [7] used population, and population and economic growth values, respectively, from the IPCC SRES scenarios [71] as well as GCM-based climate change projections to simulate domestic, industrial and agricultural water use volumes at the river-basin scale into the 2070s and 2080s. Shen et al. [90] used SRES scenario population and economic growth values and GCM-based climate projections to simulate water use values at national levels to 2075. Other models, like GCMs and Regional Climate Models (RCMs), typically include simple representations of land-surface hydrological processes but omit water withdrawals and other socio-economic factors – see, for example, Arora and Boer [13], Manabe et al. [67] and Betts et al. [17]. A few IA models, such as TARGETS [87] and WorldWater [94], have included water resources as one of their many components but the majority have omitted water-related variables.

At the river-basin scale, a variety of numerical water management models has been developed to explore feedbacks between society and water resources systems. Like the global models, these basin-scale models have focused either on connections between water quantity and quality, or water availability and water use. Many such models have dealt with water resources systems primarily from a natural sciences perspective: Xu et al. [114], Tidwell et al. [102], Langsdale et al. [61], Madani and Marino [64], Williams et al. [110], Bagheri et al. [14] and Prodanovic and Simonovic [80] linked hydrological and water use models, while Paredes-Arquiola et al. [75] and Zhang et al. [115] recently combined water quantity and quality models. The first group of models simulated feedbacks between water use – based on assumed population growth trends – and water availability. Xu et al. [114] forecasted annual water demands and the likelihood of water scarcity to 2030 in the Yellow River basin, China, for a variety of water demand and supply options. Tidwell et al. [102] developed an annual-scale model of the Middle Rio Grande basin, USA, for community-based water resources planning. Langsdale et al. [61] connected river flows from climate and hydrological models with dynamic, monthly water demands in the Okanagan basin, Canada. Madani and Marino [64] investigated the effects of current water management policies, population growth and climate change in the Zayandeh-Rud basin, Iran, on the environmentally-sensitive Gav-Khuni Swamp. Williams et al. [110] developed an educational model at a yearly scale that connects historical flows in several of Arizona's rivers with dynamic water use models to evaluate policies for greater water-use efficiency. Bagheri et al. [14] evaluated the effects of post-disaster water provision policies in Bam, Iran, on water availability through a "system crisis index" similar to the "water resources vulnerability index" discussed in Section 3.3.2. Prodanovic and Simonovic [80] studied possible effects of hydrological extremes in the Upper Thames River basin, Canada, with a coupled hydrological and socio-economic model at the sub-daily to monthly scale. Unusually, three urban- to basin-scale models – those of Madani and Marino [64], Bagheri et al. [14], and Prodanovic and Simonovic [80] – simulated explicit feedbacks between variables related to population, the local economy and water resources. In these models, population change was represented either as a function of water availability and economic welfare [64,14], or water, employment and housing availability [80]. Dynamic feedbacks then caused population changes to affect local water resources in turn. Omitting dynamic socio-economic models, the second group of natural-sciences models focused on connections between water use and quality, and projected socio-economic behavior exogenously from historical trends. The nonlinear optimization model that Paredes-Arquiola et al. [75] developed for the Jucar basin, Spain, simulated a wide variety of water quantity and quality variables realistically at a monthly scale in a large, heavily-used semi-arid basin. A second nonlinear optimization model developed by Zhang et al. [115] for the Jiaojiang basin, China, focused on wastewater treatment, included both quantity and quality variables and ran at a daily scale.

As opposed to these natural sciences-based models, other studies at the river-basin scale have investigated water supply and demand feedbacks from an economic perspective. These models, however, generally omit water quality, and use scenarios of climate, hydrological and population change. Fernandez and Selma [38] developed an irrigation model using the system dynamics methodology for the Segura basin, Spain, that simulates feedbacks between agricultural cropland expansion, profitability, water availability and water quality (salinity). Hurd et al. [55] used nonlinear optimization allocation and impact models (Water-AIM) in four representative US watersheds to estimate national-level economic impacts of climate change on water resources. Tanaka et al. [99] developed an economic optimization model that minimizes operating and scarcity costs for water supply in California and used two climate change-based hydrological scenarios to project water demand to 2100. Iglesias and Blanco [56] developed a nonlinear optimization model for Spain, applied to four basins, and determined irrigation technology sensitivity to water price – higher prices led to less water consumption and lower farm income through the adoption of more efficient technologies and, increasingly, of dryland farming.

3. Model description: ANEMI

ANEMI represents an attempt to model nonlinear feedbacks between water resources and socio-economic and environmental systems both explicitly and dynamically. Therefore, changes in variable values in each of nine – climate, carbon cycle, economy, land-use, agriculture, population, natural hydrological cycle, water use and water quality – linked system dynamics models [81,97,95] affect model variables in other sectors at each time step from 1960 to 2100. ANEMI is described in detail in Davies and Simonovic [29]; however, a brief comparison of the model with other similar models and a description of its capabilities and limitations, a summary of the methodology and model structure, and a description of recent updates follow.

3.1. Description of ANEMI and comparison with other models

In integrated assessment terms, ANEMI is horizontally-integrated and links climate change, water resources and other physical and socio-economic issues "to sketch an integrated conception of sustainable development" [76, p. 594]. It is intended for policy evaluation, or for answering "what if?" questions [103], rather than for policy optimization. Because of a focus on broad socio-economic and environmental feedbacks, model development followed a "downward approach" [96] toward system modeling: we explored first-order controls, or key processes, in representing real-world behaviors and then expanded the model step-wise to improve its ability to reproduce observations. Thus, ANEMI reproduces the major structural attributes of its eight key components at a global-aggregate level and links them together to represent the larger society-biosphere-climate system at an annual scale [27–29]. Unlike models programmed in structural languages, "high-level simultaneities" – in which the avoidance of circular references means that a set of variables must be pre-set and other variable values calculated hierarchically from those set values – do not pose a problem for the ANEMI model. Circular references, or "feedbacks", are the main focus of system dynamics modeling. Further, many feedbacks that are treated as external quantities by either natural science- or economically-based models, such as economic output and industrial emissions for natural sciences-based models, climate change and the carbon cycle for economic models and population growth for both model types, are modeled explicitly in ANEMI. Of particular interest are the water use and water quality sectors, which are strongly linked to the behavior of the other model sectors.

As described in detail in Davies and Simonovic [29], many integrated assessment models, climate-economy models and water supply and demand models have both higher spatial resolution and greater complexity in individual sectors than ANEMI has. For example, IMAGE [3,72] operates at high resolution on a global grid and includes a variety of important socio-economic and natural components and processes. WaterGAP2 [5,7] simulates both water demand and supply for individual river basins. RICE [74] and GCAM [60,112] divide the world into eight and fourteen economic regions, respectively. Since modeling involves trade-offs, each of these models has a different focus and policy-applicability. ANEMI is intended to provide a balanced, comprehensive approach towards global change and water resources modeling and to serve as a framework for further integrated assessment efforts. Thus, it contains a relatively simple representation of the macro-economic system that is common to climate-economy models like DICE [74,73] and FREE [39,40], and represents economic growth, industrial emissions and carbon tax effects endogenously, but lacks the technological detail of larger IA models like GCAM and IMAGE and so cannot simulate changes in primary and secondary energy supply and demand. Unlike GCAM and IMAGE, however, ANEMI includes water supply and demand like the more complicated WaterGAP2 model and also simulates surface flows and water scarcity, like WaterGAP2, Macro-PDM [11] and WBM [108]. ANEMI, TARGETS and WorldWater [94] also simulate water quality issues, although with several key differences. As compared with ANEMI, TARGETS models nutrient cycles and human health but prescribes economic behavior in scenario-form, while WorldWater models persistent pollution and population growth in greater detail but neglects climate change, nutrient cycles and land-use. Further, like LPJmL [86], GCWM [92] and H08 [50], ANEMI simulates both blue and green water use [84,83] for agricultural (blue water withdrawal and consumption, and green water consumption) and domestic and industrial (blue water withdrawal and consumption) purposes. Finally, ANEMI is not alone in focusing at a global, annual scale on intersectoral feedbacks – DICE, FREE, TARGETS, WorldWater and World3 [69] also have a global scale, and models like DICE and GCAM have multi-year temporal resolutions. At the basin-scale, water resources models typically have monthly resolutions, but some, like Xu et al. [114], Tidwell et al. [102] and Williams et al. [110] also have an annual resolution. Despite their low resolution, such models are useful because they show the effects of long-term changes on average conditions.

In terms of model capabilities, ANEMI can simulate effects of uncertainties in the climate and carbon systems, such as changes in climate sensitivity parameters or soil Q_{10} factors [51], or the land use and economic sectors, such as the rate of land use change or the total factor productivity. It can also show the broader effects of alternative carbon tax levels and population growth mechanisms, and a variety of water resources-related policies and uncertainties. The water sectors – surface flow, water use, and water quality – simulate changes in many key water resources variables: total surface flow, surface water availability, domestic, industrial and agricultural (both blue and green [37]) water withdrawal and consumption volumes, reservoir evaporation losses, treated and reused wastewater volumes, groundwater extraction and desalination volumes and a measurement of water scarcity, called water stress. Their values depend on water sector processes but also on dynamic connections to other sectors, such as the climate, economy and population sectors. Many of their associated parameters can be adjusted to show the effects of uncertainties or alternative management policies. See Davies and Simonovic [28] for the full list of adjustable parameters and Davies and Simonovic [29] for a list of experiments undertaken with the model. Recent updates described below also allow the model to simulate agricultural production and land use for various dietary configurations and their effects on water quality and availability. Analysis of the output from ANEMI is relatively straightforward, as shown in Section 4, and individual simulations take roughly two minutes on a desktop computer. This simulation speed makes possible the comprehensive Monte Carlo sensitivity analyses conducted with the model [27,29].

The fast simulation runs and analytical tractability of ANEMI are partly products of the global-aggregate and annual scales used in the model, which have important implications for the interpretation of simulation results, of course. Specifically, precipitation volumes at a global scale may vary little from one year to the next but can change significantly at regional scales, while surface water withdrawal and consumption volumes, and water quality and treatment levels, differ significantly from one region to the next. In other model sectors, global GDP figures mask significant national and regional differences; land use changes and their distributions have important effects on local and regional carbon emissions, the hydrological cycle, and population distributions; and the list goes on. Clearly, scale is important. The horizontal integration in ANEMI therefore represents a trade-off: while many disciplinary models focus on the scale of individual hydrological, nutrient cycle, climatic or socio-economic characteristics, ANEMI focuses on the dynamic feedbacks that connect them. The reasoning is as follows. Society and the natural environment are connected through a feedback loop: changes to the climate and natural systems will require society to adapt, and its adaptation efforts will affect the global environment in turn. This interplay between natural and socio-economic systems determines the entire system's evolution and makes the representation of the corresponding feedbacks critical to the development of appropriate adaptation and mitigation strategy [29]. Most models focus on specific components of the earth-system and assume the behavior of other components by applying projected trends, output of other models, or reanalysis data to "drive" the behavior of the component in question. In other words, most models understand connections between natural and socio-economic systems by separating them through modeling techniques [93]. In contrast, ANEMI links humans directly with hydrological and other systems, models the world as coupled and non-stationary, represents the system as complex and adaptive, and *synthesizes*, by modeling over a long time-frame, as well as *analyzes* – see Fig. 5 in Wagener et al. [109]. We cannot answer all water-related questions with ANEMI, but we can gain greater insight into the driving mechanisms and their feedbacks with water resources.

Gleick [47] recently observed that humans are now capable of planetary-scale disruptions of the ecosystems that sustain us, and that we have reached this point by various simultaneous exponential increases in population, energy use and industrial emissions, economic activity and water use. ANEMI models these disruptions, their nonlinear nature and their broader consequences explicitly. As such, it can inform the debate on the "global water crisis" [57] by illustrating the effects of key feedbacks and identifying areas that may benefit from further study. Researchers and the rest of society learn by analogy – the approaches that work in one location offer suggestions for approaches that work in others. ANEMI's global scale and concentration on the effects of feedbacks provide a new approach to understanding the causes and effects of a "global crisis", but its structure and the types of experiments conducted with the model can also inform existing regionally-focused approaches.

3.2. Modeling methodology and model structure

ANEMI uses a well-established modeling methodology called "system dynamics" that has many similarities with IA modeling. As a worldview, system dynamics asserts that a system's structure and its associated feedbacks give rise to its observed behavior. Most real-world events are then a consequence of the internal structure of a potentially larger, and perhaps unrecognized, system. Thus, observed events are not external to the systems they affect but stem instead from unforeseen interactions between system components. This recognition entails a shift in perspective from one-way to circular causality that has profound implications for modeling and for worldview more generally. "In effect, it is a shift from viewing the world as a set of static, stimulus–response relations to viewing it as an ongoing, interdependent, self-sustaining, dynamic process" [81, p. 118].

In practice, system dynamics models aim to represent real-world structures and processes through nonlinear feedbacks, stocks and flows, and delays. Using first-order ordinary differential equations, solved numerically, system dynamics models can incorporate both empirical and mechanistic approaches [35] and produce comprehensive simulation models quickly and easily [80]. Rather than improve mechanistic representations of individual processes, system dynamics models are intended to increase understanding of the unpredictable effects of feedbacks between sub-systems, whose behavior would otherwise be assumed or ignored. Thus, individual model components are often relatively simple and replicate the behavior of key variables or processes [35], with model improvements occurring analogously to the "downward approach" [96] described above. Modeling and simulation work in combination: modeling determines structure and clarifies ideas and simulation then reveals unexpected behaviors and clarifies their causes [43]. The analysis of simulation results provides insight into the system and, where model results are unexpected, can expose the importance of overlooked feedbacks, or can reveal errors either in the simulation model's mathematical execution and modeling logic or in the "mental models" we use to understand complex systems [97,98]. System dynamics has been applied successfully to water resources systems at catchment to global and daily to annual scales [94,100,35,61,64,107,110,14], climate change and energy-economy modeling [39,31,40,23], and a variety of real-world problems related to policy analysis, economics, biology, medicine, industrial engineering and urban planning, for example [1,58,35,62].

Fig. 1 shows ANEMI's basic structure, with sector names in bold type and feedbacks as arrows that connect the individual sectors into a set of linked, closed-loop structures. The resulting feedbacks are a critical feature of the model and mean, in practical terms, that the values of key variables in one sector affect the values of variables in other sectors at *each time step* of a simulation. These closed loops cause model behavior to emerge from the interactions between different sectors rather than from input data or driving functions – dynamic behavior is then a result of *endogenous feedbacks* [97]. An endogenous approach is well-suited to an exploration of feedback-effects between elements of the overall system, because it allows an attribution of system behavior to real-world characteristics and to the effects of particular feedback relationships within the model. Positive or negative signs associated with each arrow in Fig. 1 indicate the direction of change one model component imposes on the next. Positive relationships represent change in the same direction, where an increase/decrease in one sector causes an increase/decrease in the next sector. Negative relationships mean that change occurs in the opposite direction, so that an increase/decrease in one sector causes a decrease/increase in the next sector. Furthermore, each arrow connecting two model sectors bears the name of the sectoral element whose change causes a related change in the next model sector. For example, the connection between the carbon and climate sectors, called "atmospheric CO_2", indicates that an increase in the global atmospheric carbon dioxide (CO_2) concentration causes an increase in the global temperature, the key output of the climate sector. Davies and Simonovic [29] provide a detailed description of the model as well as its key equations.

ANEMI has been validated through comparisons with real-world observations and with results from other models. It has performed well overall, as described in Davies and Simonovic [29]. Specifically, temperature changes produced by the climate sector are conservative but lie within the spectrum of values from recent complex climate models, as reported by Forster and Gregory [44]; carbon and hydrological cycle performances compare well with the data from Keeling and Whorf [59], Berthelot et al. [16], Chahine [21], Gleick [46] and Shiklomanov [91]; and water use, economic

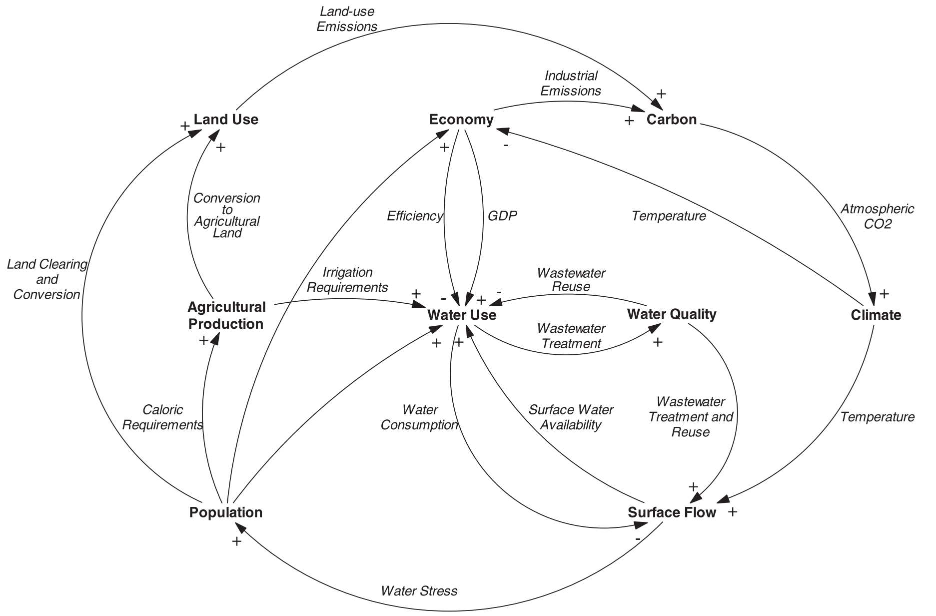

Fig. 1. The structure of ANEMI: model components and their feedbacks. (Adapted from [27].)

growth, and population growth values closely match the data from Shiklomanov [91], Maddison [65,66], the World Bank [101], and the United Nations [104]. Simulated future values of the key variables compare well with the values produced by other models, and with projections from governmental and international institutions. Some further information on model performance is provided in Davies and Simonovic [29], while the details of model validation are presented in Davies [27] and Davies and Simonovic [28].

3.3. Recent updates: agricultural production, green water and water stress

The version of ANEMI presented here differs from the version in Davies and Simonovic [29] in several important ways: (1) the new version models agricultural production and expansion explicitly, (2) differentiates between green and blue water consumption [83] in global agriculture, and (3) includes the water quality effects of rainfed-cropland runoff on water stress levels. Addition of green water provides a more balanced assessment of the effects of agriculture on water resources – the previous version omitted water quality effects of rainfed agriculture and thus exaggerated the negative effects of irrigation. The new agricultural production sector represents the effects of shifts in diet explicitly on land and water requirements. Finally, the new water stress indicator differentiates between domestic, industrial and agricultural water uses, and incorporates the pollution effects of rainfed agriculture. With these changes, ANEMI can now be used to assess effects of different crop productivity values, changes in global nutrition levels, shifts in animal product consumption and variable dilution requirements for water pollution. This paper describes recent additions to ANEMI and applies the model to understand connections between global water resources and socio-economic and environmental change.

The remainder of this section describes recent changes to ANEMI to incorporate agricultural production and expansion, green water, and the new water stress indicator. Data sources for the following calculations include the Food Balance Sheets, yield information and annual harvested areas of FAOSTAT [41], yield information and crop water productivity (g m^{-3}) values from GCWM [92] and pasture and fodder area and productivity values from Bouwman et al. [18], since the FAO Food Balance Sheets do not include fodder and pasture information. Simulated values from the model are comparable with green water consumption values in Rost et al. [86], Siebert and Döll [92], Hanasaki et al. [50], Rockström et al. [85] and Postel [77], while crop yield, harvested area and pasture area are similar to Siebert and Döll [92], Monfreda et al. [70], FAOSTAT [41] and Bouwman et al. [18].

3.3.1. Agricultural production and green water

In ANEMI, agricultural production and green water consumption are calculated in several stages. First, daily per capita caloric consumption (kcal capita^{-1} day^{-1}, or kcal cap^{-1} d^{-1}) – the driver of agricultural crop production and thereby green water consumption – is broken into three energy-content components: food-crop, animal feed-crop and "other" crop (seed, fuel and processed) production. Fodder crops and pasture-based production are simulated separately because of their different yields and water requirements. In equation form, the total per capita caloric consumption (CC) is,

$$CC = DC + IC \tag{1}$$

where DC is the direct consumption (kcal cap^{-1} d^{-1}) by humans and IC is the indirect use of agricultural energy for feed, fodder, grazing and "other" purposes. The inclusion of indirect consumption is important because FAO data show that animal-feed and "other" crops currently comprise roughly 50% of the energy in non-fodder crops; they are therefore critical to the green water consumption calculations presented later in this section. The direct consumption is,

$$DC = (1 - \alpha_p)FC_c + \alpha_p \cdot AP_c \tag{2}$$

where α_p is the animal-product fraction of the diet, FC_c is the food-crop consumption per capita and AP_c is the animal product (meat, milk, eggs and so on) consumption per capita – both are measured in kcal cap^{-1} d^{-1}. DC and α_p are prescribed to allow exploration of the effects of alternative diets on land use and water resources, while FC_c and AP_c are calculated as functions of the overall diet. Direct consumption, DC, increased from 2195 to 2796 kcal cap^{-1} d^{-1} from 1961 to 2007 [41] and is assumed to grow to 2900 kcal cap^{-1} d^{-1} in 2100, a level that would virtually eliminate malnutrition [85]. The animal products component, α_p, rose from 0.15 to 0.17 from 1961 to 2007 [41] and is assumed to reach 0.195 by 2100. These values are fairly conservative, since 27% of

US calories came from animal products in 2007 [41] and Bouwman et al. [18] assumed animal products would make up 25% of the global diet by 2030, for example. The indirect consumption of agricultural energy has four components,

$$IC = AFC + OC + AF + PG \tag{3}$$

where *AFC* is animal feed-crop consumption, *OC* is other-crop consumption, *AF* is animal fodder and *PG* is pastoral grazing. All four terms are measured in Exacalories per year (or Ecal yr^{-1}, where 1 Ecal = 10^{15} kcal). Eq. (3) is not used directly in the model; it is provided here simply for illustrative purposes.

Second, the per capita figures of Eq. (2) are converted to global crop-energy production values (in Ecal yr^{-1}) through multiplication with the global population, which is simulated in the population sector of ANEMI. In a similar fashion, the animal feed- and "other" crop consumption values of Eq. (3) are given by,

$$AFC = \alpha_f \cdot AP_c \cdot P \cdot \mathrm{d/yr} \tag{4}$$

$$OC = \varphi[(FC_c \cdot P \cdot \mathrm{d/yr}) + AFC] \tag{5}$$

where α_f is the animal feed-energy input to the animal product-energy output (for human consumption) ratio, φ is the fraction of "other" crops in agricultural non-fodder production, *P* is the global population and d/yr is the number of days per year. Historically, the feed-crop ratio has decreased as the proportions of cereals, roots and tubers, and sugar crops in feed have increased relative to higher-energy animal products, and as animal production has shifted from ruminants to poultry and pork [41]. Thus, the value for α_f decreases from roughly 3.5:1 to 2.6:1 from 1960 to 2007, while the fraction in 2100 is assumed to be slightly lower at 2.5:1 – different values can be tested for their effects on model behavior. The percentage of "other" crops in the total agricultural energy production has risen steadily from 1960 to the present, from roughly 25% to 33% [41]. The fraction of "other" crops, φ, is therefore set to 0.34–0.44 for 1960–2000 and is assumed to rise to 0.55 by 2100. If food- rather than fodder crops are increasingly used for biomass production, the assumed year-2100 value is potentially quite conservative. The sum of *DC*, *AFC* and *OC* increases from 4.6 Ecal in 1961 to 13.6 Ecal in 2007.

Third, the required agricultural cropland is determined based on crop yields from irrigated and rainfed land, which are calculated as,

$$Y_I(t) = \int y(t) \cdot dt \tag{6a}$$

$$y(t) = \upsilon(t-1) \cdot Y_I(t-1) \tag{6b}$$

$$Y_R = 0.6 Y_I \tag{7}$$

where Y_I is the yield on irrigated land (Gcal ha^{-1}), *y* is the rate at which that yield increases (Gcal ha^{-1} yr^{-1}), υ is the prescribed growth in crop yield (fraction yr^{-1}) and Y_R is the yield on rainfed land (Gcal ha^{-1}). Crop yields, υ, rose by roughly 2.25% yr^{-1} from 1960 to 1990 and then at 1.1% yr^{-1} from 1990 to 2007 [77,9] thereafter, υ is assumed to decline to zero by 2100. Initial globally-averaged yield values of Y_I = 6.25 Gcal ha^{-1} and Y_R = 3.75 Gcal ha^{-1} in combination with the "nutritive factors" from the FAO [42] give irrigated and rainfed yields of 13.6 Gcal ha^{-1} and 8.2 Gcal ha^{-1} in 2000, for an average yield of 10.2 Gcal ha^{-1}. This average yield is in line with global values of 9.6 Gcal ha^{-1} [41] and 10.3 Gcal ha^{-1} [92]. To the best of our knowledge, this second publication is the only one that provides specific regional and global values for irrigated versus rainfed yields, and the irrigated yields provided are for crops grown on irrigation-equipped fields, with the actual irrigated yields approximately 20% higher than those they provide.

Based on Bouwman et al. [18] and Siebert and Döll [92], ANEMI also simulates the growth of fodder crops and pastures as animal feed, according to,

$$ACT = \alpha_{IO} \cdot AP \tag{8}$$

where *ACT* is the total consumption of agricultural energy from feed, fodder, and grazing (Ecal yr^{-1}) by animals, *AP* is the animal product consumption (Ecal yr^{-1}; $AP = AP_c \cdot P \cdot \mathrm{d/yr}$) and α_{IO} is the prescribed ratio of energy input to animal product output. This parameter declines as in Bouwman et al. [18] from 14.1:1 to 10.4:1 from 1970 to 2030 – values for 1960 and 2100 are selected to follow this trend. Pastoral grazing (*PG*) is assumed to account for 35% of caloric intake of animals in 1960, less than 33% in 2000 and 28% by 2100. The pastoral percentages were chosen, given the assigned feed-input to animal product-output ratio, to match both the decreasing trend of feed-energy from grazing in Bouwman et al. [18] and the fodder production in 2000 from Siebert and Döll [92]. Fodder crop yield rises in the same fashion as the irrigated yield in Eqs. (6a) and (6b), while pastoral yield is assumed to increase at half the rate of agricultural crops, representing the less intensive management of pasture land. Initial yields are selected as 16 Gcal ha^{-1} and 0.65 Gcal ha^{-1}. Fodder production is calculated from,

$$AF = AP[\alpha_{IO}(1-\alpha_g) - \alpha_f] \tag{9}$$

where *AF* is the fodder production (Ecal yr^{-1}) and α_g is the pastoral grazing fraction with the values given above. Multiplication of the irrigated and rainfed yields of step three with the required energy production values of step two gives a total food-, feed- and "other" crop area of 1162 Mha in 2000 (262 Mha irrigated, 900 Mha rainfed), which is close to the FAOSTAT value [41] of 1135 Mha. Including fodder production, according to Eq. (9), gives a total harvested area of 1290 Mha to match the values of Siebert and Döll [92] and Monfreda et al. [70] at 1305 and 1290 Mha, respectively. In 1960, with lower crop productivity, the harvested areas without and with fodder, respectively, are 974 Mha and 1157 Mha. The pasture area is 3145 Mha in 1970 and rises to 3460 Mha in 1995 to approximately match the figures of 3268 Mha and 3415 Mha in Bouwman et al. [18].

Finally, virtual water contents (VWC; in m^3 Gcal^{-1}) are combined with global crop-energy values (Ecal yr^{-1}) to determine green water consumption values (km^3 yr^{-1}). The calculation is as follows. Virtual water contents for each of the major crop groups – cereals, roots and tubers, sugar crops, vegetables and fruits, oil crops, and pulses – were calculated from crop production and nutritive factor values [41,42] and crop water productivity (CWP; in g m^{-3}) factors [92]; forage values were omitted since they are not provided in the Food Balance Sheets. The crop-group virtual water contents and the weighted average of energy-production by crop group – in 2000, crop-energy was provided by cereals (63%), oil crops (15%) and roots and tubers (6%), for example – gives an aggregate virtual water content of roughly 420 m^3 Gcal^{-1}. Omitting more water-efficient fodder crops, aggregate virtual water content values from Siebert and Döll [92] and Rockström et al. [85] are 435 m^3 Gcal^{-1} and 530 m^3 Gcal^{-1}, respectively. Combining the virtual water contents with the crop-energy values then gives an equation for green water consumption (C_g) as,

$$C_g = \omega_c(FC + AFC + OC) + \omega_f(AF + PG) \tag{10}$$

where ω_c and ω_f are the virtual water content values of food-, feed- and "other" crops, set to 450 m^3 Gcal^{-1}, and of fodder crops and pasture, set to 250 m^3 Gcal^{-1}. Eq. (10) results in a green water consumption of 1650 km^3 in 1960 that rises to 4720 km^3 in 2000; blue water consumption over the same period rises from 1040 km^3 to 1800 km^3, which matches values in Shiklomanov [91] but is higher than consumption values in Siebert and Döll [92], Rost et al. [86]

and Hanasaki et al. [50]. The same authors, as well as Rockström and Gordon [84], calculated green water consumption values in 2000 of 5505 km^3, 7242 km^3, 7820 km^3 and 5400 km^3, respectively. Although virtual crop-water contents are likely to decrease over time through agricultural research – Rockstrom et al. [85] assumed that water productivity improves in developing countries from 1770 m^3 $tonne^{-1}$ in 2002 to 1200 m^3 $tonne^{-1}$ in 2050, for example – they are kept constant in ANEMI in the reference simulation.

3.3.2. Water stress

Water stress, a key variable in ANEMI, has no single, commonly accepted definition [82]. Here, water stress is defined as "a measure of the degree of pressure put on water resources (including its quantity and ecosystems) by users of the resources, including municipalities, industries, power plants and agricultural users" [8, p. 353]. The most commonly used indicator of water stress is the "Falkenmark indicator", a per capita measure [82]. The "Water Resources Vulnerability Index" used here, which is calculated as the ratio of the annual withdrawals-to-availability (wta), is also used widely, particularly in water resources modeling [11,82]. In equation form, water stress can be calculated simply as,

$$wta = W/R \tag{11}$$

where W is the surface water withdrawal volume and R is the surface runoff. Both are measured in $km^3\,yr^{-1}$. Water stress (*wta*) values of 0.2 indicate "mid-stress", while values of 0.4 and higher indicate "severe stress" [8,82]. Vörösmarty et al. [108] used a similar scale. According to Arnell [11], water scarcity can have significant effects on socio-economic and environmental systems, where an indicator values of 0.2 or higher suggests that water stress is likely to limit development.

Rijsberman [82, p. 7] observes that "water quality ought to be another major variable in an assessment of water scarcity, [since] fresh water may become polluted as it flows downstream and become *de facto* unusable...". However, although several authors note its importance [53,45,94,36,15], the environmental and socio-economic effects of water quality on water scarcity have not been modeled at a large scale. To include water quality effects on surface water availability, ANEMI modifies the "withdrawals-to-availability" ratio of Eq. (11). The rationale is as follows. Wastewater results from domestic water use, manufacturing processes, irrigation projects, and rainfed cropland, and pollutes receiving waters. Pollution makes those receiving waters unsuitable for further use in many cases, especially for drinking-water supply. Specifically, every cubic meter of contaminated wastewater discharged into water bodies and streams renders eight to ten cubic meters of pure water unsuitable for use, according to Shiklomanov [91]. Dabrowski et al. [26] found generally lower dilution requirements for South African agriculture. Based on the assumption that nitrogen, phosphorus and pesticide losses are roughly 10%, 5% and 1%, respectively, of the applied amounts, they quantified dilution requirements for agricultural runoff from five major crops and calculate ratios of roughly 0.8:1 (maize) to over 15:1 (cotton) for water quality:water quantity requirements. For three major crops (maize, wheat and sugar cane), they found ratios between 0.8:1 and 1.7:1, but their values may be somewhat conservative: for example Schlesinger [89] calculated global nitrate and total nitrogen losses to surface runoff of 15% and 23%, respectively, based on studies in the Northeastern United States. Boyer et al. [19] modeled a global-average riverine nitrogen export of 25%, based on inputs from synthetic fertilizers, atmospheric deposition, natural fixation and lightning. Liu et al. [63] reported leaching and erosion losses of 16% and 15%, respectively, of the total global nitrogen input. Chapagain et al. [22] calculated that, on a worldwide basis, roughly 19% of the virtual water content of cotton is for dilution of nitrogen applied as fertilizer. Overall, uncertainty in global nitrogen fluxes is high: few values are known to better than ±20% and many have uncertainties of ±50% and higher [48].

3.3.3. Water quality

ANEMI quantifies water quality effects as follows. Through its dilution requirements, untreated wastewater increases the amount of surface water appropriated for human use by the volume of clean surface water required to dilute both the polluted volume of blue water and the polluted runoff from rainfed cropland. To incorporate these water quality effects on water stress levels requires two steps. First, ANEMI reduces domestic, industrial and agricultural withdrawals by the amount of clean, reusable (post-treatment) water returned to surface sources, and then applies use-specific (domestic, industrial and agricultural) blue water dilution factors to calculate an effective blue water withdrawal. As described in Davies and Simonovic [29], all domestic wastewater is assumed to be polluted [46]. For industrial uses, manufacturing is assumed to pollute surface water but the cooling requirements of thermoelectric power generation are neglected [105]. Non point source pollution from agriculture is assumed to be untreatable [78,24]. Second, ANEMI models the volume of runoff from rainfed cropland and pasture as an area-weighted fraction of the total runoff from the land surface, and then applies a "green water" dilution multiplier to calculate dilution requirements for agricultural chemical use on rainfed land. Three equations, for domestic, industrial, and agricultural water use, are the result,

$$W_{eff_d} = C_d + \delta_d R_{p_d} \tag{12a}$$
$$W_{eff_i} = C_i + \delta_i R_{p_i} \tag{12b}$$
$$W_{eff_a} = C_a + \delta_a R_{p_a} + \delta_r R_r + \delta_g R_g \tag{12c}$$

where the three W_{eff} terms are the effective withdrawals ($km^3\,yr^{-1}$) for domestic (d), industrial (i), and agricultural (a) purposes, the C terms are water consumptions ($km^3\,yr^{-1}$), the δ terms are dilution multipliers, and the R_p terms are the polluted return flow volumes for blue water, and for rainfed cropland, R_r, and pasture, R_g ($km^3\,yr^{-1}$). Both consumption and return flow volumes are dynamic, while the blue water dilution multipliers are reduced from 9 [91] to 7.5 – by 16% to incorporate the self-cleaning mechanisms of rivers [113] – and the two green water dilution multipliers, for rainfed cropland (δ_r) and pasture (δ_g), are set to 1 based on Dabrowski et al. [26] and 0.1 (assumed). Because best values for dilution multipliers are unknown, the selected values are the subjects of sensitivity analyses, below. Finally, the sum of the W_{eff} terms is the surface water withdrawal volume, W ($km^3\,yr^{-1}$) from Eq. (11), so that the water stress equation can be rewritten as,

$$wta = \left(\sum_{d,i,a} W_{eff}\right)/R \tag{13}$$

The result of the Eq. (13) is that a larger volume of untreated wastewater makes a smaller volume of clean water available for domestic, industrial, and agricultural purposes. The runoff value, R, is the total annual surface runoff, which several other authors [79,94,5] reduce to an "accessible runoff" volume, since the whole volume is inaccessible. We do not take this approach because the combination of reduced runoff and withdrawal increases through dilution requirements results in water stress values well over *wta* = 1.0. Thus, a higher value of water stress is calculated here than in Eq. (11); however, the experiments undertaken below show how Eq. (13) offers an improvement on the standard definition by explicitly incorporating the effects of water pollution on water availability. Davies and Simonovic [28,29] and Davies [27] provide a detailed description of the model's water sectors and a fuller analysis of the effects of Eq. (13) on simulated behavior.

4. Model use and water management

This section describes applications of ANEMI to water resources management, in terms of water stress definitions, wastewater treatment and reuse, expansions in the irrigated area and changes in the human diet. The first part describes the analytical approach used in this section, while the second presents the behavior of the reference simulation against which the experiments are compared. The third and largest component of the section analyzes a set of five simulation runs.

4.1. Analytical approach: feedback tracing

To understand the causes of differences in model behavior between the reference simulation and the experiments in the following sections, we use an analytical approach called "feedback tracing". Feedback tracing has two basic forms: a standard, reverse causal-tracing approach and a more complicated feedback-isolating approach. Both find the causes of differences in key variable values between the experimental and reference simulations by following chains of interconnected variables. To understand the principle of the approach, consider the following example. Assume that the water stress variable, *wta*, on the left-hand side of Eq. (13) begins with the same values in the reference simulation and an experimental simulation that increases the population growth rate. The parameter changes used for this population experiment will cause the water stress values to diverge gradually between the simulations so that wta_{expt} will differ noticeably from wta_{ref} after some time, *t*. According to Eq. (13), possible causes are differences in the numerator (the "effective withdrawal", or W_{eff}), denominator (the "surface runoff", or *R*), or both values. Further, the two variables, W_{eff} and *R*, that determine the value of water stress (*wta*) are products of several other calculations. Thus, the number of variables that could be responsible for the divergence in *wta* values in the reference simulation and experiment one grows significantly as we trace backwards from one equation to the next.

In most cases, one right-hand side variable differs considerably between the reference and experimental runs while the other right-hand side variables have relatively similar values. In the example above, the effective withdrawal comes from the "water use" sector, while the surface runoff is from the "hydrological cycle"; parameter changes for the agricultural water-use experiment would be expected to change the "effective withdrawal" more than the global surface runoff. Then the standard feedback analysis approach applies. Assume that the differences between $W_{eff_{ref}}$ and $W_{eff_{expt}}$ are significantly larger than the differences between R_{ref} and R_{expt}. Feedback analysis then begins with the variables on the right-hand side of Eq. (2), W_{eff}, and checks for the variable or set of variables that differs most from the reference to the experimental simulation. Again, the difference between the base and experimental values of one variable, W_{eff_d}, W_{eff_i} or $W_{eff_{a'}}$, is generally considerably larger than that of the other two variables. The analysis continues backwards through right-hand side variables until the differences between their reference and experimental simulations are negligible, or $X_{ref} \cong X_{expt}$, at which point the causal tracing stops. With the point of divergence identified, any differences between the variables in the reference simulation and experiment one must have occurred in the variables already examined. The calculations for these variables can then be checked for sensitivity to the imposed parameter changes. In this case, feedback analysis allows us to determine whether change in domestic, industrial or agricultural use with population growth affects the water stress value most.

The second form of feedback analysis, feedback isolation, becomes necessary when causality is difficult to determine. In such cases, several different feedback loops contribute to the divergence in variable values between the selected experiments and no single cause dominates. To isolate feedbacks, individual loops are severed so that only one feedback of interest is allowed to operate in a simulation run, while other key variables are held to a form of behavior common to all experiments. A set of supplementary experiments is run where each focuses on a different feedback. The isolation approach allows the identification of the major feedback, or set of feedbacks, responsible for the simulated behavior from a potentially large group of minor feedbacks. However, it should be used with caution, as it severs links between variables – and thus alters model structure – that could produce important feedback-effects with other model components.

Regardless of the feedback analysis approach chosen, both reveal not just the direct cause but the reason for the differences between simulations: they provide insight into the functioning of the system, and help to identify the dominant structures and feedbacks in the model. When the modeled system contains a small number of feedbacks, feedback analysis is straightforward. However, in dynamically complex systems where possibly thousands of feedbacks – in the case of ANEMI's water stress, for example – affect model behavior through nonlinear equations, the approach becomes especially powerful since important variables can be identified quickly, while variables with relatively similar values between simulation runs can be eliminated as causes.

4.2. The reference simulation

Generated using the initial model configuration, the reference simulation serves as the basis of comparison for other experiments. It shows a doubling of the global population from 1960 to 2000 and then a slower increase to 2100. The simulated population numbers from 1960–2000 match United Nations figures [104] quite closely (see Table 1), being roughly 20 million too high in 2000.

Other key variables also increase over the 140-year simulation period. The modeled temperature rises from 1960 to the present, but at roughly half the rate suggested by Vinnikov et al. [106] from 1978 to 2004 because of the relatively small sensitivity of the climate sector, which is based on Harvey and Schneider [52]. In the carbon cycle sector, the atmospheric carbon dioxide levels are close to those of Keeling and Whorf [59] with a value of 374 ppm in 2000. Values for net primary productivity (NPP), which is the net flux of carbon dioxide from the atmosphere into green plants, compare well with both observed and simulated figures from the literature, with a 2000 value of 64 Gt C yr^{-1}. The economic output produced by the model from 1960 to 2005 matches figures from Nordhaus and Boyer [74], Maddison [66] and the World Bank [101] closely, with a 1960 value of \$5.45 $\times 10^{12}$ yr^{-1} in 1990 US dollars at market exchange rates and a 2005 value of \$30.0 $\times 10^{12}$ yr^{-1}, while the difference in cumulative industrial emissions between the model simulation and the data [68] is only 2 Gt C, or 1.0%, over 40 years.

Table 1
UN data versus ANEMI values (in 10^9 people).

Year	1960	1965	1970	1975	1980	1985	1990	1995	2000	2005
UNESA [101]	3.02	3.34	3.70	4.08	4.45	4.86	5.30	5.72	6.12	6.51
ANEMI	3.02	3.37	3.73	4.12	4.51	4.91	5.32	5.73	6.14	6.54

In the water sectors, the total available surface water decreases first to 2000, as a result particularly of evaporation from the surfaces of reservoirs [91], and then increases from 2000 to 2100 as climate change and the related enhancement of the hydrologic cycle compensate [54]. Furthermore, in all three water use sectors – domestic, industrial and agricultural – surface water withdrawals increase strongly to 2000 and then remain basically constant over the next century, while surface water consumption grows quickly from 1960 to 2000 and then rises more slowly over the next hundred years. These behaviors result from technological change and from the simulated rates of increase in efficiency, reservoir surface-evaporation and wastewater treatment and reuse. Simulated values for global domestic, industrial and agricultural water withdrawal and consumption volumes match historical figures from Shiklomanov [91] very closely. For example, in 1995, the last year for which observed figures are available, simulated total withdrawals and consumption are 3774 and 2084 $km^3\,yr^{-1}$, respectively, while the observed figures are 3788 and 2074 $km^3\,yr^{-1}$ – see Fig. 2.

Reference simulation values into the future are lower than those of Shiklomanov [91]; instead, at 4346 and 2417 $km^3\,yr^{-1}$ by 2025, they are closer to values from Cosgrove and Rijsberman [25] and Alcamo et al. [6] at 4300 and 2100 $km^3\,yr^{-1}$, and 4091.5 $km^3\,yr^{-1}$, respectively. In terms of water scarcity, water stress levels peak around the present and then decrease over the next hundred years as wastewater treatment and reuse programs become more common.

4.3. Insights into water resources management from ANEMI

Using the feedback-tracing approach described above, this section describes and analyzes five sets of experiments that focus on wastewater treatment and reuse, irrigation expansion, animal product consumption and the effects of alternative dilution factor values. The first two experiments focus on blue water resources, and demonstrate the effects of wastewater treatment and reuse on blue water resources. In many areas of the world, wastewater is already treated, which reduces or even eliminates the contamination effect of wastewater on pure receiving waters. Increasingly, water-scarce regions, such as the Middle East, Southern Africa and parts of the United States, are also reusing treated wastewater to reduce the demand for surface water withdrawals [45,46]. In contrast, wastewater is untreated in other areas and its discharge into surface waters causes pollution. Regardless, studies of water scarcity have tended to disregard water pollution effects because water quality has been seen either as a local concern without global impact, or modeling water quality at the global scale has been seen as too difficult because of a lack of information. We show here that large-scale modeling is possible and that the effects of dilution requirements on simulated behavior are considerable. In the model's reference run, higher levels of water scarcity drive improvements in wastewater treatment and reuse infrastructure. Two experiments illustrate these effects: experiment one, "low treatment, no reuse", allows neither wastewater treatment nor reuse (beyond the fraction treated in 2000) and so illustrates the model-wide effects of the greatest volume of water pollution, while experiment two, "high treatment, no reuse", allows wastewater treatment without reuse and so simulates the broader effects of wastewater reuse.

Experiments three and four include both blue and green water resources, and investigate the expansion of irrigated agriculture and the effects of more animal products in the human diet. In the real world, irrigation is responsible for a large proportion of the total blue water withdrawn from surface water resources per year, accounting for 67% of the global withdrawal and 87% of the global water consumption [33]. Irrigated agriculture is an important source of food but is also expensive and damaging to water resources and the environment [78]. After considerable expansion in the 1950s-1970s, irrigation growth has slowed noticeably in both developed and developing countries because the best sites have generally already been developed [78]. Expansion of the irrigated area into the future is therefore unknown, and is assumed to grow slowly in the reference simulation, according to the approach taken by Simonovic [94]; however, because Shiklomanov [91] suggests that the global irrigated area will grow considerably in the future to meet the needs of a growing population, experiment three explores an expansion of the global irrigated area. In terms of experiment four, animal production is resource intensive. It requires significant agricultural inputs from feed-crops, fodder and pastoral grazing, as well as large volumes of water and agricultural chemicals. According to Bouwman et al. [18], the ratio of feed-energy in to animal product-energy out (from meat, dairy products, eggs and so on) was over 14:1 in 1970 – and other authors like Wirsenius [111] find even higher ratios – although it has fallen somewhat since. Experiment three, "irrigation expansion", and experiment four, "more animals", therefore investigate the effects of an increased irrigated area and of increased animal-product consumption on the balance of blue and green water consumption, on water stress levels and on the rest of the society-biosphere-climate system.

Finally, the set of simulations in experiment five investigates the effects of different "green water" dilution requirements for rainfed agriculture. Since appropriate values for fertilizer and pesticide dilution factors are unknown, as explained above, experiment five shows the model results for several different sets of parameter values.

4.3.1. Representation of policy options

Each model sector contains both variables and parameters. Variables change in value over time according to mathematical equations and experimentation could, in theory, involve changes

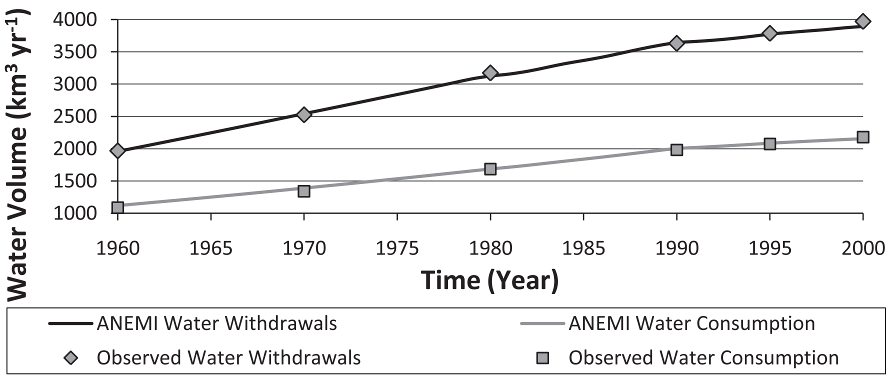

Fig. 2. ANEMI versus observed water withdrawal and consumption values [91].

in these equations to determine their influence on model behavior. However, since such changes would modify the model's structure, and could therefore yield a fundamentally new model, they are not considered here. Instead, various socio-economic policy options are simulated through changes in appropriate model parameters – this approach to policy simulation affects behavior without changing structure.

Parameters are one of four types: initial values, constants, switches and exogenous variables. Initial value parameters give starting values for model variables, constants retain a single value over the course of the simulation, switches enable or disable a certain type of model behavior and exogenous variables vary over time in a fixed, pre-set manner. Changes in initial values can have significant effects on model behavior, but are of less interest here because they concern the effects of uncertainty in a starting-point rather than altering the dynamic behavior of the model. The last three parameter types are therefore of more interest. Modifications to constant values generally relate to model sensitivity – the values of constants are typically changed to determine the degree to which the model reacts to that change. Switches enable or disable critical feedbacks in the model in a binary "on–off" fashion. Finally, exogenous variables represent input to the model that changes over time in a predetermined fashion. In this case, the process driving the change is not modeled explicitly and the real-world elements involved in determining change in these exogenous variables consequently exist outside the system boundaries.

Experiments one to five involve the modification of a small subset of parameters in the socio-economic sectors of the model, as shown in Table 2. Specifically, "low treatment, no reuse" changes two water quality sector constants that represent delays in establishing both domestic and industrial wastewater treatment facilities so that less wastewater is treated in this experiment than in the reference case. Furthermore, both "low treatment, no reuse" and "high treatment, no reuse" set the switch related to wastewater reuse to zero (off) so that no treated wastewater is reused over the simulation period. "Irrigation expansion" doubles the "irrigation expansion multiplier" after the year 2000 so that the simulated irrigation area matches Shiklomanov [91] until 2000, but then rises at twice the reference rate thereafter. "More animals" raises the fraction of meat in the human diet linearly from 0.172 in 2007 to 0.25 by 2030 [18] and holds that value to 2100, whereas the reference run has a linearly rising consumption from 0.172 in 2007 to 0.195 in 2100. Finally, experiment five sets the "green crop water dilution factor" and "green pasture water dilution factor" parameters to a range of values to show the effects of larger and smaller dilution requirements.

4.3.2. Effects of policies on model variables

In each experiment, the imposed parameter changes directly affect certain key variables and indirectly affect others through dynamic feedbacks. Where an equation contains a parameter altered in one of the experiments, that change has a direct effect on the model variable on the left-hand side. For example, the parameter changes in the "low treatment, no reuse" experiment affect the rate of change in the fraction of domestic or industrial wastewater treated, df_{cl_x}/dt (in fraction yr^{-1}), through the parameter that represents the delay in establishment of further treatment, τ_{fcl_x}(in yr). For these and related terms, the subscript x pertains to domestic ($x = d$) or industrial ($x = i$) wastewater. In equation form,

$$\frac{df_{cl_x}}{dt} = \frac{wta \cdot f_{cl_x}}{\tau_{fcl_x}} \tag{14}$$

where wta is the water stress from Eq. (13), is the fraction (from 0 to 1) of domestic or industrial wastewater currently treated, and the other terms are as defined above. This equation causes the treated fraction to rise exponentially to a maximum value, set optimistically to 100%, at a rate determined by the water stress and delay terms. An alternative logistical growth approach for domestic and industrial treatment and wastewater reuse, described in Davies [27], yields a smoother transition from treatment growth to a steady state value. Although the model is sensitive to the differences between the exponential (Eq. (14)) and logistical growth approaches, the experiments listed in Table 2 produce far larger changes in model behavior. For example, the difference in population, GDP, global temperature, water withdrawals and water stress in 2100 are 200 million, $\$1.5 \times 10^{12}$ yr^{-1}, 0.006 °C, 272 km^3 yr^{-1} and 0.046, respectively. Similarly, parameter changes in the "irrigation expansion" experiment affect the growth of the irrigated area directly. The equation is,

$$\frac{dI}{dt} = (\mu \cdot \varepsilon_{base}) \cdot I \tag{15}$$

where dI/dt is the expansion in the irrigated area (ha yr^{-1}), μ is the irrigation expansion multiplier manipulated in the experiment, is the base expansion rate (*fraction* yr^{-1}) and I is the current irrigated area (ha).

In contrast, where the change in a variable's value comes through feedbacks that connect it to one or more other variables, the change can be indirect. For example, Eq. (14) shows not only the direct effect described above but also a feedback effect: higher levels of water pollution, introduced through the water stress variable, wta, drive efforts to improve treatment. Therefore, at the same time that water stress is influencing the degree of wastewater treatment through Eq. (14), the fraction of wastewater treated feeds back to affect water stress through Eq. (13). Causation occurs simultaneously through model feedbacks, and so the resulting changes in behavior can be difficult both to foresee and understand. In such cases, simulation is particularly useful.

4.3.3. Blue water experiments: wastewater treatment and reuse

The reference results of the model are compared here against results from the two blue-water experiments, "low treatment, no reuse" and "high treatment, no reuse". In examining the simulation results, note that IA models are intended to improve insight into key real-world processes and characteristics, rather than to provide predictions. Therefore, despite the provision of quantitative

Table 2
Experimental configuration and associated changes to ANEMI parameters.

Experiment title	Objective: "*Show effects of…*"	Parameter changed	Parameter reference value	Experimental value (post-2000)
1. Low treatment, no reuse	*High volumes of polluted water*	Domestic treatment Delay	15 yr	10^8 yr
		Industrial treatment delay	40 yr	10^8 yr
		Wastewater reuse switch	1 (on)	0 (off)
2. High treatment, no reuse	*Greater wastewater reuse*	Wastewater reuse switch	1 (on)	0 (off)
3. Irrigation expansion	*Larger irrigated area*	Irr. expansion multiplier	1	2
4. More animals	*Greater animal product consumption*	Animal product fraction	2100: 0.195	2030: 0.25
5. Dilution requirements	*Alternative dilution requirements*	Green crop water dilution	1	0.5, 1.5, 2, *Var.*
	for rainfed agriculture	Gr. pasture water dilution	0.1	0.05, 0.15, 0.2, *Var.*

values, the important experimental results are the qualitative differences between simulations and corresponding differences in behavioral patterns.

Parameter changes in the two experiments led to the direct effects presented in Table 3. The "low treatment, no reuse" experiment showed high volumes of untreated wastewater over time and no reuse of treated wastewater. The "high treatment, no reuse" experiment had no reuse, but wastewater treatment was simulated at levels higher than in the reference run.

The experiments also demonstrate the value of a feedback-based model: almost every key variable value in the experiments differed from its reference value, whether or not that variable was directly linked to the altered parameters and variables. Such differences indicate that, while the simulated management decisions generally had strong direct effects, they also had important indirect, or feedback, effects that caused the changes in one sector to propagate throughout the model sectors (see Fig. 1). Table 4 focuses on these indirect effects, and the global population figures present a clear example: while the reference run had a final population in 2100 of 12.50 billion people – an endogenously-generated value that is similar to those in Fiddaman [39] and Alcamo et al. [2], and sits in the middle of the range of SRES projections [71] between the B2 and A2 scenarios – the values for population in the three water resource policy experiments were smaller by 720 million and 370 million people for the low and high treatment experiments, respectively.

Table 3
Direct effects of the blue water experiments on key variables.

Key variable	2000	2010	2025	2050	2075	2100
Untreated wastewater ($km^3\ yr^{-1}$)						
• Reference	860	842	766	500	269	235
• Low treatment, no reuse	885	910	978	1053	1121	1170
• High treatment, no reuse	885	885	848	722	703	727
Treated wastewater ($km^3\ yr^{-1}$)						
• Reference	342	452	612	863	946	1025
• Low treatment, no reuse	349	441	517	624	706	759
• High treatment, no reuse	349	466	647	959	1137	1229
Wastewater reuse ($km^3\ yr^{-1}$)						
• Reference	46	81	170	459	904	1025
• Low treatment, no reuse	0	0	0	0	0	0
• High treatment, no reuse	0	0	0	0	0	0

4.3.3.1. Blue water withdrawals. In ANEMI, blue water use and reuse for domestic, industrial, agricultural and reservoir purposes sum to the total surface water withdrawal. Specifically, domestic withdrawals depend on the global population, the economic gross domestic product (GDP), technological change, desalination and wastewater reuse, industrial withdrawals depend on GDP, electricity production, technological change and wastewater reuse, and agricultural withdrawals depend on the irrigated area, water requirements per hectare, technological change, climate change, fossil groundwater use and wastewater reuse. In equation form, these withdrawals, W_d, W_i, and W_a, in km^3 yr^{-1}, are calculated as,

$$W_d = z \cdot DSWI \cdot P - DS - Q_{r_d} \tag{16}$$

$$W_i = z \cdot ISWI \cdot EO - Q_{r_i} \tag{17}$$

$$W_a = z_a \beta_{base} [T_{feedback} \cdot I] - GW - Q_{r_a} \tag{18}$$

where the z terms represent technological change, $DSWI$ and $ISWI$ are the domestic and industrial structural water intensities in m^3 cap^{-1} and m^3 MWh^{-1} [5], P is the global population (people), EP is the electricity production (MWh), DS is the volume of desalinated water (km^3 yr^{-1}), the Q_r terms represent treated wastewater reuse in each sector (km^3 yr^{-1}), β_{base} is the base specific water intake (m^3 ha^{-1}), $T_{feedback}$ is the effect of climate change on evaporation rates (a multiplier) and GW is the withdrawal of non-renewable groundwater resources (km^3 yr^{-1}). Both DS and GW are negligible volumes at well less than 1% of the total. See Davies and Simonovic [28,29] for a more detailed description of Eqs. (16)–(18).

In terms of experimental results, the blue water withdrawal – see Table 4 – in the reference run was 4372 km^3 yr^{-1} in 2100, while the withdrawals for the low and high treatment experiments were higher by 959 and 991 km^3 yr^{-1}, or 22% and 23%, respectively. In both experiments, the majority of these additional withdrawal volumes were for irrigated agriculture, Eq. (18). Where

Table 4
Feedback effects of the blue water experiments on key variables.

Key variable	2000	2010	2025	2050	2075	2100
Population (10^9 people)						
• Reference	6.14	6.94	8.10	9.82	11.28	12.50
• Low treatment, no reuse	6.13	6.94	8.07	9.69	10.91	11.78
• High treatment, no reuse	6.13	6.94	8.08	9.75	11.09	12.13
Temperature change (°C)						
• Reference	0.30	0.42	0.62	0.99	1.39	1.83
• Low treatment, no reuse	0.30	0.42	0.62	0.98	1.38	1.80
• High treatment, no reuse	0.30	0.42	0.62	0.98	1.38	1.81
Atmospheric [CO_2] (ppm)						
• Reference	374	395	430	499	585	693
• Low treatment, no reuse	374	395	430	498	582	683
• High treatment, no reuse	374	395	430	498	583	688
Economic output ($\$10^{12}\ yr^{-1}$)						
• Reference	26.55	33.23	43.18	60.85	80.62	102.83
• Low treatment, no reuse	26.53	33.19	43.07	60.19	78.36	97.46
• High treatment, no reuse	26.53	33.19	43.08	60.47	79.47	100.06
Blue water withdrawals ($km^3\ yr^{-1}$)						
• Reference	3894	4130	4346	4406	4258	4372
• Low treatment, no reuse	3940	4210	4512	4854	5131	5331
• High treatment, no reuse	3940	4210	4513	4859	5146	5363
Water stress (–)						
• Reference	0.35	0.36	0.35	0.31	0.28	0.29
• Low treatment, no reuse	0.36	0.37	0.39	0.41	0.43	0.45
• High treatment, no reuse	0.36	0.37	0.37	0.35	0.36	0.37

irrigation projects received 615 $km^3\,yr^{-1}$ of reused water in the reference simulation, they were forced instead to rely on additional surface water withdrawals in the two experiments. As a result, agricultural water use was almost 24% higher, or to rephrase, by 2100 the reuse of treated wastewater in the reference run reduced the use of clean surface water by 24% annually.

In the domestic and industrial sectors, wastewater reuse likewise reduced total withdrawals while also allowing relatively greater water use. For example, although the reference run consumed slightly more water than the low and high treatment experiments, surface water withdrawals were higher for both experiments throughout the simulated period. Specifically, domestic withdrawals in 2100 were 985, 1028 and 1057 $km^3\,yr^{-1}$ for the reference run, "low treatment, no reuse" and "high treatment, no reuse" respectively, while the actual water use volumes – the first term on the right-hand side of Eq. (16) – were 1087, 1028 and 1057 $km^3\,yr^{-1}$. Wastewater reuse reduced domestic water withdrawals by more than 100 $km^3\,yr^{-1}$. Finally, by 2100 the industrial withdrawal volumes in the two experiments were 303 and 306 $km^3\,yr^{-1}$ higher, respectively, than the reference value of 630 $km^3\,yr^{-1}$, again because treated wastewater could not be reused.

4.3.3.2. Water stress, and wastewater treatment and reuse. Water stress is a key variable in ANEMI because of its connections to variables in both the water sectors and the rest of the model. Water stress affects population growth and population then dominates the socio-economic behavior of the model, causing changes in economic output, industrial and land-use emissions and global surface temperature, as described in Davies and Simonovic [29].

The differences in water stress levels in Fig. 3 between the three simulations are directly related to wastewater treatment and reuse. Wastewater treatment in the "high treatment, no reuse" experiment reduced the untreated volume by 443 $km^3\,yr^{-1}$ in 2100 from its low treatment value, with clear effects on water stress. Furthermore, as compared with the reference simulation, the higher water stress level in the high treatment experiment drove greater establishment of wastewater treatment facilities – 204 $km^3\,yr^{-1}$ more wastewater was treated. This feedback effect is apparent in Eq. (14), where a higher water stress (*wta*) value causes the treatment fraction, f_{cl}, to grow more quickly. (This feedback can also have the opposite effect, however: an apparent increase in water availability reduces water stress and so decreases the rate of establishment of new wastewater treatment facilities.)

Wastewater reuse then accounted for the majority of the remaining difference between the "high treatment, no reuse" experiment and the reference run. By 2100, wastewater reuse in the reference run amounted to 1025 $km^3\,yr^{-1}$ and averted the pollution of 615 $km^3\,yr^{-1}$ of blue water for irrigation, as well as 410 $km^3\,yr^{-1}$ for domestic and industrial purposes. Since irrigation water is untreatable and requires considerable dilution in ANEMI, this difference in the volume of agricultural returnable water had a large effect on water stress levels. Differences between the simulations in the total withdrawal volumes accounted for the remaining gap in water stress levels.

Fig. 4 illustrates the effects of wastewater treatment and reuse feedbacks on total wastewater volumes. The three solid lines show the total volumes of wastewater generated in the reference run and in the low and high treatment experiments. The dashed lines show that the treated wastewater volume rose over time, the untreated volume decreased in the reference simulation and the total volume of wastewater decreased through reuse. The untreated volume in the "high treatment, no reuse" experiment behaved analogously to the reference untreated volume but decreased less over time since wastewater was not reused. The total wastewater reuse in the reference run eventually matched the total treated wastewater volume; this treatment to reuse relationship can be changed easily in light of new information. Finally, the two treated-wastewater curves show the effects of water stress feedbacks on treatment, as described above: the wastewater treatment volume in the high treatment case clearly rose faster than in the reference run, because of both its higher water stress values and its higher wastewater volume.

4.3.3.3. Broader effects of the wastewater treatment and reuse policies. Other feedbacks also influence model behavior. As stated above, scarcer water resources in the blue water experiments reduced the population growth rate from its reference behavior. These lower populations then caused economic output to diverge, from \$97.46 × $10^{12}\,yr^{-1}$ in 2100 for "low treatment, no reuse" up to \$102.8 × $10^{12}\,yr^{-1}$ for the reference run (see Table 4). Lower population also led to less surface temperature change and lower atmospheric CO_2 concentrations in the two experiments, because fewer people coupled with less economic activity caused less environmental change.

Many variables exhibited less change than population, but their variation remains important from a water resources perspective. For example, if the difference in industrial withdrawals between the simulations depended only on wastewater reuse, the experimental withdrawals would be 303 $km^3\,yr^{-1}$ higher than the reference value. Yet, the actual differences were found to be 298 and 300 $km^3\,yr^{-1}$ higher for the low and high treatment experiments – differences that resulted from a feedback with the economic sector of the model. The industrial structural water intensity [5] depends on GDP per capita, which was actually greater for the two experiments than for the reference run; the macro-economic Solow growth model explains this effect [27]. As a result, the industrial sector required slightly less water for its purposes in the two experiments than in the reference simulation and so higher water stress led indirectly to slightly higher industrial efficiency.

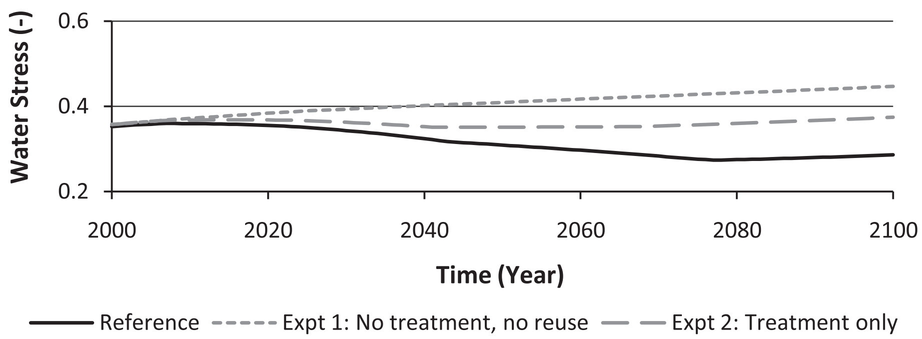

Fig. 3. A comparison of water stress values in the reference simulation and experiments one and two.

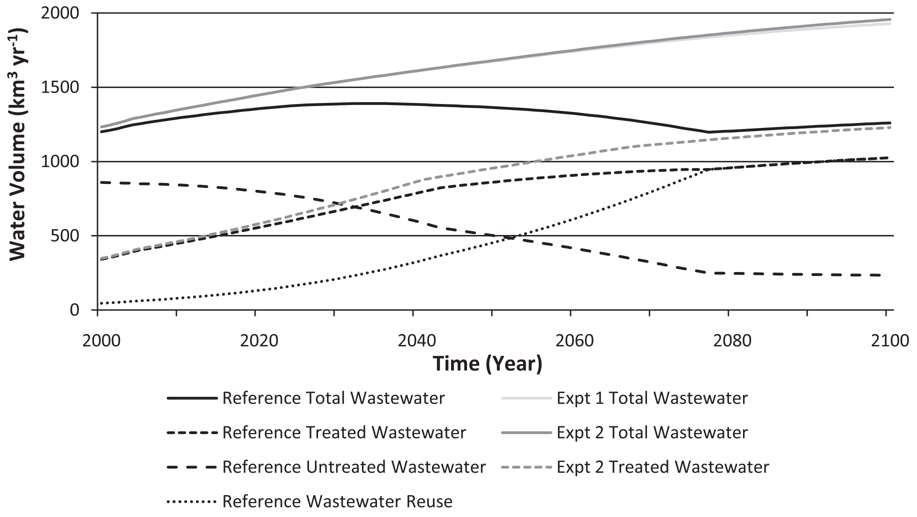

Fig. 4. Total wastewater, wastewater treatment, and wastewater reuse volumes ($km^3\ yr^{-1}$).

Surface water availability also varied between the reference run and the two experiments since climate change drove differences in the hydrological cycle. Specifically, because of the small differences in final global average surface temperatures from Table 4 of 1.80 °C, 1.81 °C and 1.83 °C in the low and high treatment experiments and the reference simulation, respectively, the associated available surface flows in 2100 were 42,418, 42,427 and 42,437 $km^3\ yr^{-1}$. In other words, in ANEMI neither the effective withdrawals nor the base hydrological conditions remained the same in each simulation because of both the water-sector and broader-model feedbacks.

4.3.4. Blue and green water experiments: irrigation, dietary changes, and dilution factors

ANEMI simulates blue and green water feedbacks associated with agriculture; the top lines of Table 5 compare the direct effects of the experiments. In the "irrigation expansion" experiment, an increase in the μ parameter of Eq. (15) produced significant increases in the irrigation area. The "more animals" experiment prescribed greater animal product consumption at levels from Bouwman et al. [18].

The direct effects of more irrigation in the "irrigation expansion" experiment included greatly-increased blue water use over the course of the simulation, with a withdrawal almost 1500 $km^3\ yr^{-1}$ higher in experiment three than in the reference simulation. However, greater irrigation also reduced green water consumption and the agricultural area by 2100. Specifically, as the irrigated area rose to 584 Mha, the rainfed area fell to 890 Mha from its reference value of 1261 Mha because of irrigation's higher productivity. Greater blue water consumption also reduced green water consumption by 1564 $km^3\ yr^{-1}$. In the "more animals" experiment, greater consumption of animal products drove the conversion of 115 Mha, or 7%, more natural land to cropland, and without substantial increases in pastoral productivity, required approximately 1350 Mha more pasture land than in the reference run. Further, greater animal product consumption required an additional 1549 $km^3\ yr^{-1}$ green water consumption to grow 6.3 Ecal, the equivalent of 1566 $kcal\ cap^{-1}\ d^{-1}$, more agricultural and pastoral energy in 2100. In the reference simulation, agricultural energy production for all crop, fodder and grazing purposes is already 25 Ecal higher in 2100 than in 2000.

More blue water use and greater animal-product consumption had broader feedback effects as well, as shown in Table 5. Water stress values rose significantly from the reference value of 0.29–0.37 and 0.31 because of higher blue-water and green-water dilution requirements, respectively – see Eq. (12c). Thus, in the reference simulation, the effective blue water withdrawal was 4548 $km^3\ yr^{-1}$ as compared with 8467 $km^3\ yr^{-1}$ for "irrigation expansion", while the reference and "more animals" green-water dilution requirements for rainfed cropland and pasture were 5794 and 1810, and 6196 and 2282 $km^3\ yr^{-1}$, respectively.

The higher blue-water withdrawal and "green returnable flow" and their associated dilution requirements had far-reaching consequences. As the irrigated area grew in "irrigation expansion" and drove higher water stress values, the rate of population growth fell in comparison with the reference run results. Furthermore, higher water stress values meant that the maximum domestic and industrial treatment fractions were reached earlier – see Eq. (14) – in the "irrigation expansion" experiment than in the reference simulation: in 2041 versus 2044, and in 2068 versus 2075, respectively. In the case of wastewater reuse, the respective maximum reuse fractions were reached in 2070 and 2078. In other words, higher water stress in "irrigation expansion" drove the earlier implementation of wastewater treatment and reuse programs but water pollution was already dealt with to the extent possible by 2070, making no further treatment or reuse possible. Water stress continued to rise as a result.

Higher water stress values in the "more animals" experiment had the same effects but to a lesser degree because of the lower green water dilution requirement. However, the water stress equation is quite sensitive to the green-water dilution factors used. Fig. 5 shows the effects of different values on water stress and the corresponding values of the standard water stress definition from Eq. (11), which omits water quality considerations. Five additional simulations, called experiments 5-1, 5-2 and 5-3 use cropland and pasture runoff-dilution factors of 0.5 and 0.05, 1.5 and 0.15, and 2.0 and 0.2, respectively, while "standard water stress" shows the value from Eq. (11), where availability is set to 37% of the annual renewable volume. Experiment 5-4 makes the dilution factor a function of crop yield – of the form $\delta = c(Y/Y_0)$, where c is a constant set to 0.5 and 0.05 for cropland and pasture, respectively, and Y and Y_0 are the current and initial yields – to represent the effects of intensifying agricultural production on water resources.

The "irrigation expansion" and "more animals" experiments highlight important trade-offs in global agriculture. Since irrigated agriculture currently occupies about 17% of all agricultural land [91] and supplies roughly 40% of the world's food [32], the expansion of irrigation would seem a sound approach for reducing world

Table 5
Blue and green water experimental results.

Key variable	2000	2010	2025	2050	2075	2100
Irrigated area (Mha)						
• Reference	263	279	305	337	363	392
• Irrigation expansion	263	296	354	433	503	584
• More animals	263	279	305	337	363	392
Dietary fraction of animal products						
• Reference	0.167	0.173	0.176	0.183	0.189	0.195
• Irrigation expansion	0.167	0.173	0.176	0.183	0.189	0.195
• More animals	0.167	0.182	0.233	0.250	0.250	0.250
Population (10^9 people)						
• Reference	6.14	6.94	8.10	9.82	11.28	12.50
• Irrigation expansion	6.14	6.94	8.09	9.76	11.10	12.16
• More animals	6.14	6.94	8.09	9.78	11.16	12.29
Blue water withdrawals ($km^3\,yr^{-1}$)						
• Reference	3894	4130	4346	4406	4258	4372
• Irrigation expansion	3894	4294	4789	5172	5353	5864
• More animals	3894	4130	4342	4375	4221	4366
Green water consumption ($km^3\,yr^{-1}$)						
• Reference	4730	5807	7184	9570	11,862	14,051
• Irrigation expansion	4730	5689	6853	8912	10,817	12,487
• More animals	4730	5972	8330	11,204	13,511	15,600
Harvested area (Mha)						
• Reference	1288	1340	1360	1404	1490	1653
• Irrigation expansion	1288	1328	1325	1330	1371	1473
• More animals	1288	1362	1491	1557	1624	1768
Water stress (–)						
• Reference	0.354	0.359	0.351	0.309	0.276	0.286
• Irrigation expansion	0.354	0.369	0.375	0.349	0.335	0.366
• More animals	0.354	0.363	0.372	0.332	0.297	0.308

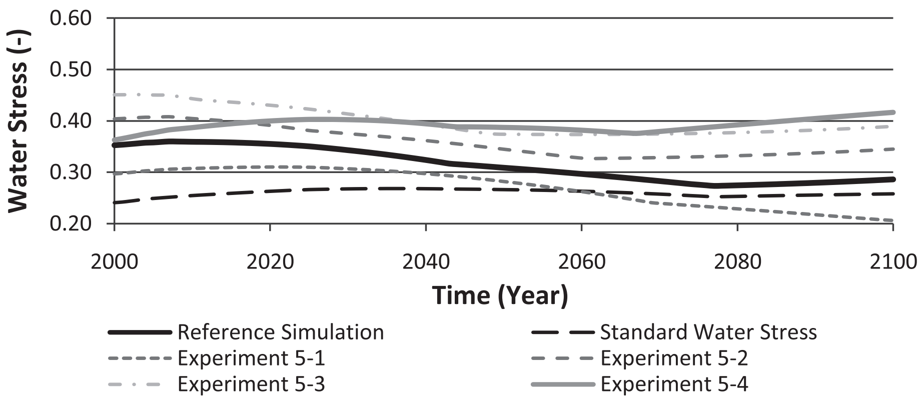

Fig. 5. Effects of changes in dilution requirements on water stress.

hunger, and possibly even for reducing the human environmental footprint. However, the results of "irrigation expansion" show that the polluting effects of irrigation may outweigh its food-production benefits. In the "more animals" experiment, a greater fraction of animal products in the human diet increased the required harvested and pasture areas, green water consumption and water pollution levels. Clearly, dilution water volumes can strongly influence the calculated water stress level, but only a few studies [91,94,22,26] have attempted to quantify dilution requirements at any scale. Since real-world dilution requirements remain uncertain and model results are sensitive to the selected values, the results of experiments one to four should be considered primarily in terms of their qualitative rather than quantitative behaviors. A greater number of watershed and river basin scale studies that investigate the connections between crop yields, soil management and fertilizer application techniques, and nutrient and pesticide concentrations in surface runoff from both irrigation projects and rainfed agriculture would help in this regard.

5. Conclusions

Water resources systems are particularly difficult to model at a global level because of the number of different real-world systems to which they are connected. Furthermore, their components change over time in generally unpredictable fashions that have historically given rise to inaccurate water use projections, for example [46]. These inaccuracies arise because population change, economic growth, technological progress, land-use change, precipitation and runoff levels, surface temperature change and a great many more factors are related to water resources systems, and they all interact through feedbacks in complex, nonlinear ways that confound traditional modeling approaches. In most global change fields, insights into comparably large-scale, complex feedback-based systems have come through the integrated assessment modeling approach.

Comprehensive, feedback-based modeling approaches towards water resources policy development, although uncommon [94], are desirable for several reasons. They represent water resources systems realistically within their broader context [109], clarify cause-and-effect relationships and test important assumptions. Most importantly, since the society-biosphere-climate system is characterized by interdependent, self-sustaining and dynamic processes, rather than by static, stimulus–response relationships [81], a greater understanding of its behavior will come from a modeling approach that includes these characteristics [93].

Of course, recognition of the importance of feedback has driven the development of global hydrological models like WaterGAP2 [5], WBM [108], Macro-PDM [10] and H08 [49], vegetation and agricultural models like LPJmL [86], GCWM [92] and WATERSIM [30], and IA models like WorldWater [94] and TARGETS [53]. However, ANEMI differs from most other global-scale hydrological and water resources models in several important ways. It incorporates dynamic, interdependent representations of both socio-economic and natural systems, represents systemic feedbacks explicitly, includes endogenous representations of population, economic growth, global surface temperature and the carbon cycle, and focuses on connections between water quantity, water quality and natural surface flow. The model has clear limitations, including its global resolution and annual timescale, and would benefit from changes to the population sector and to land-use – such modifications are planned for future versions of the model [29]. However, its global scale and concentration on feedback effects provide a new approach to understanding the causes and effects of a "global crisis" [57], while model simulations can inform existing regionally-focused approaches.

The five water resources experiments examined in this paper showed several benefits of a feedback-based modeling approach. Specifically, a comparison of the reference run with the low and high treatment experiments demonstrated the water resources- and broader benefits of wastewater treatment and reuse programs, while the "irrigation expansion" and "more animals" experiments showed the blue and green water effects of an expansion of irrigation and of shifts toward greater consumption of animal products. The additional dilution sensitivity simulations, experiments 5-1, 5-2, 5-3 and 5-4, investigated the effects of changes in the dilution factors for runoff from rainfed agricultural land. The methodological approach used, feedback tracing, followed cause-and-effect relationships from one sector to another through the model, and improved insight into the behavior of both the modeled and real-world systems.

In the case of "low treatment, no reuse" and "high treatment, no reuse", feedback tracing showed that water quality problems related to limited wastewater treatment and reuse could cause major water scarcity, which could then affect the broader socio-economic system with consequences even for the global population. The reference simulation, in contrast, illustrated the considerable benefits of implementing extensive wastewater treatment and reuse programs. The "irrigation expansion" experiment suggested that irrigation schemes have significant beneficial effects, but that their impacts on water quality and on broader socio-economic systems must also be considered. The "more animals" experiment showed that greater consumption of animal products not only affects the global agricultural area, but also water resources systems, and demonstrated the sensitivity and value of a water stress definition that incorporates water quality as well as water quantity. Finally, the additional dilution sensitivity simulations, experiments 5-1, 5-2, 5-3 and 5-4, demonstrated how relatively small changes in the dilution factor can have large effects on the water stress level. Together, these experiments clearly showed that feedbacks have important effects – both expected and unexpected – on modeled- and real-world behavior.

Decisions as to appropriate wastewater treatment and reuse levels, expansions in irrigated agriculture and shifts in dietary composition in reality involve short- and long-term socio-economic trade-offs, since the degree of global change over the next one hundred years is uncertain and its effects on the global economy are unclear, as are the feedbacks that connect them. Management strategies can therefore be tested in the model for their direct and indirect effects, while model sensitivities can suggest areas for further study. When surprises occur, they are useful: researchers learn something new by tracing the causal relationships that led to the result. Furthermore, in the case that the effects are unlikely, or even possibly wrong, a feedback-based model can help to reveal the shortcomings in the current level of understanding that created the model component in question, and then allow a test of assumptions. ANEMI serves as an example of the kind of learning tools available, and the analyses described above demonstrate its value in improving understanding of the society-biosphere-climate feedbacks that determine the whole system's evolution.

Acknowledgements

This work was funded by two generous National Science and Engineering Research Council (NSERC), Canada, graduate scholarships awarded to E.G.R. Davies and an NSERC Strategic Grant awarded to Prof. S.P. Simonovic. We also thank the four anonymous reviewers whose comments have improved the paper.

References

[1] Ahmad S, Simonovic SP. Spatial system dynamics: new approach for simulation of water resources systems. J Comput Civ Eng 2004;18(4):331–40.
[2] Alcamo J, Kreileman GJJ, Bollen JC, van den Born GJ, Gerlagh R, Krol MS, et al. Baseline scenarios of global environmental change. Global Environ Change 1996;6(4):261–303.
[3] Alcamo J, Kreileman GJJ, Krol MS, Zuidema G. Modeling the global society-biosphere-climate system: Part 1: Model description and testing. Water Air Soil Pollut 1994;76(1–2):1–35.
[4] Alcamo J, Vörösmarty CJ, Naiman RJ, Lettenmaier DP, Pahl-Wostl C. A grand challenge for freshwater research: understanding the global water system: editorial. Environ Res Lett 2008;3(010202). doi:10.1088/1748-9326/3/1/010202.
[5] Alcamo J, Döll P, Henrichs T, Kaspar F, Lehner B, Rösch T, et al. Development and testing of the WaterGAP 2 global model of water use and availability. Hydrol Sci J 2003;48(3):317–37.
[6] Alcamo J, Döll P, Henrichs T, Kaspar F, Lehner B, Rösch T, et al. Global estimates of water withdrawals and availability under current and future "business-as-usual" conditions. Hydrol Sci J 2003;48(3):339–48.
[7] Alcamo J, Flörke M, Märker M. Future long-term changes in global water resources driven by socio-economic and climatic changes. Hydrol Sci J 2007;52(2):247–75.
[8] Alcamo J, Henrichs T. Critical regions: a model-based estimation of world water resources sensitive to global changes. Aquat Sci 2002;64:352–62. doi:1015-1621/02/040352-11.
[9] Alston JM, Beddow JM, Pardey PG. Agricultural research, productivity, and food prices in the long run. Science 2009;325:1209–10.
[10] Arnell NW. A simple water balance model for the simulation of streamflow over a large geographic domain. J Hydrol 1999;217:314–35.
[11] Arnell NW. Climate change and global water resources. Global Environ Change 1999;9:S31–49.
[12] Arnell NW. Climate change and global water resources: SRES emissions and socio-economic scenarios. Global Environ Change 2004;14:31–52.
[13] Arora VK, Boer GJ. Effects of simulated climate change on the hydrology of major river basins. J Geophys Res – Atmos 2001;106(D4):3335–48.
[14] Bagheri A, Darijani M, Asgary A, Morid S. Crisis in urban water systems during the reconstruction period: a system dynamics analysis of alternative policies after the 2003 earthquake in Bam – Iran. Water Resour Manage 2010;24(11):2567–96.
[15] Bagheri A, Hjorth P. A framework for process indicators to monitor for sustainable development: practice to an urban water system. Environ Dev Sustain 2007;9:143–61.
[16] Berthelot M, Friedlingstein P, Ciais P, Monfray P, Dufresne JL, Le Treut H, et al. Global response of the terrestrial biosphere to CO_2 and climate change using a coupled climate-carbon cycle model. Global Biogeochem Cycles 2002;16(4). doi:10.1029/2001GB001827.

[17] Betts RA, Boucher O, Collins M, Cox PM, Falloon PD, Gedney N, et al. Projected increase in continental runoff due to plant responses to increasing carbon dioxide. Nature 2007;448(7157):1037–41.

[18] Bouwman AF, van der Hoek KW, Eickhout B, Soenario I. Exploring changes in world ruminant production systems. Agric Syst 2005;84:121–53.

[19] Boyer EW, Howarth RW, Galloway JN, Dentener FJ, Green PA, Vörösmarty CJ. Riverine nitrogen export from the continents to the coasts. Global Biogeochem Cycles 2006;20(GB1S91). doi:10.1029/2005GB002537.

[20] Cai XM, Rosegrant MW. Global water demand and supply projections. Part 1. A modeling approach. Water Int 2002;27(2):159–69.

[21] Chahine MT. The hydrological cycle and its influence on climate. Nature 1992;359(6394):373–80.

[22] Chapagain AK, Hoekstra AY, Savenije HHG, Gautam R. The water footprint of cotton consumption: an assessment of the impact of worldwide consumption of cotton products on the water resources in the cotton producing countries. Ecol Econ 2006;60(1):186–203.

[23] Climate Interactive, Ventana Systems [Internet]. C-ROADS. c2009 [cited 2010 November 25]. Available from: <http://climateinteractive.org/simulations/C-ROADS/overview>.

[24] Corcoran E, Nellemann C, Baker E, Bos R, Osborn D, Savelli H, editors. Sick water? The central role of wastewater management in sustainable development. GRID-Arendal: United Nations Environment Programme, UN-HABITAT; 2010.

[25] Cosgrove WJ, Rijsberman FR. World water vision: making water everybody's business. London: Earthscan Publications Ltd.; 2000.

[26] Dabrowski JM, Murray K, Ashton PJ, Leaner JJ. Agricultural impacts on water quality and implications for virtual water trading decisions. Ecol Econ 2009;68(4):1074–82.

[27] Davies EGR. Modelling feedback in the society-biosphere-climate system [dissertation], Department of Civil and Environmental Engineering, The University of Western Ontario, London, Ontario, Canada; 2007.

[28] Davies EGR, Simonovic SP. An integrated system dynamics model for analyzing behaviour of the social–economic–climatic system: model description and model use guide. Report no. 59, Facility for Intelligent Decision Support, Department of Civil and Environmental Engineering, The University of Western Ontario, London, Ontario, Canada; 2008.

[29] Davies EGR, Simonovic SP. ANEMI: a new model for integrated assessment of global change. Interdiscip Environ Rev 2010;11(2/3):127–61. doi:10.1504/IER.2010.037903.

[30] de Fraiture C. Integrated water and food analysis at the global and basin level. An application of WATERSIM. Water Resour Manage 2007;21(1):185–98.

[31] de Vries BJM, van Vuuren DP, den Elzen MGJ, Janssen MA. The Targets IMage Energy Regional (TIMER) model: technical documentation. Report no. 461502024 2001, The IMAGE Project, Department of International Environmental Assessment, National Institute of Public Health and the Environment (RIVM), Bilthoven, the Netherlands; 2001.

[32] Döll P. Impact of climate change and variability on irrigation requirements: a global perspective. Clim Change 2002;54(3):269–93.

[33] Döll P, Siebert S. Global modeling of irrigation water requirements. Water Resour Res 2002;38(4). doi:10.1029/2001WR000355.

[34] Edmonds J. Comment on integrated assessment modeling of climate change. In: Nordhaus WD, editor. Economics and policy issues in climate change. Resources for the future, Washington, DC; 1998. p. 291–304.

[35] Elshorbagy A, Ormsbee L. Object-oriented modeling approach to surface water quality management. Environ Model Softw 2006;21(5):689–98.

[36] Falkenmark M. Water usability degradation – economist wisdom or societal madness? Water Int 2005;30(2):136–46.

[37] Falkenmark M, Rockström J. Balancing water for humans and nature: the new approach in ecohydrology. London: Earthscan Publications Ltd.; 2004.

[38] Fernandez JM, Selma MAE. The dynamics of water scarcity on irrigated landscapes: Mazarron and Aguilas in south-eastern Spain. Syst Dyn Rev 2004;20(2):117–37.

[39] Fiddaman TS. Feedback complexity in integrated climate-economy models [dissertation], Alfred P. Sloan School of Management, Massachusetts Institute of Technology, Boston, Massachusetts; 1997.

[40] Fiddaman TS. Exploring policy options with a behavioral climate-economy model. Syst Dyn Rev 2002;18:243–67.

[41] Food and Agriculture Organization of the United Nations [Internet]. FAOSTAT database query. c2010 [cited 2010 May 25]. Available from: <http://faostat.fao.org/site/575/DesktopDefault.aspx?PageID=575#ancor>.

[42] Food and Agriculture Organization of the United Nations [Internet]. Standard nutritive factors used in food balance sheets. c2010 [cited 2010 June 1]. Available from: <http://www.fao.org/economic/ess/publications-studies/publications/nutritive-factors/en/>.

[43] Forrester JW. Counterintuitive behavior of social systems. Technol Rev 1971;73(3):52–68.

[44] Forster PMdF, Gregory JM. The climate sensitivity and its components diagnosed from Earth radiation. J Clim 2006;19(1):39–52.

[45] Gleick PH. The changing water paradigm: a look at twenty-first century water resources development. Water Int 2000;25(1):127–38.

[46] Gleick PH. The world's water: the biennial report on freshwater resources. Washington, DC: Island Press; 2000.

[47] Gleick PH. Climate change, exponential curves, water resources, and unprecedented threats to humanity. Clim Change 2010;100:125–9.

[48] Gruber N, Galloway JN. An Earth-system perspective of the global nitrogen cycle. Nature 2008;451(7176):293–6.

[49] Hanasaki N, Kanae S, Oki T, Masuda K, Motoya K, Shirakawa N, et al. An integrated model for the assessment of global water resources – Part 1: Model description and input meteorological forcing. Hydrol Earth Syst Sci 2008;12(4):1007–125.

[50] Hanasaki N, Inuzuka T, Kanae S, Oki T. An estimation of global virtual water flow and sources of water withdrawal for major crops and livestock products using a global hydrological model. J Hydrol 2010;384:232–44.

[51] Harvey LDD. Box models of the terrestrial biosphere. In: Wigley TML, Schimel DS, editors. The carbon cycle. Cambridge, UK: Cambridge University Press; 2000. p. 238–47.

[52] Harvey LDD, Schneider SH. Transient climate response to external forcing on 10^0–10^4 year time scales. Part I: Experiments with globally averaged, coupled, atmosphere and ocean energy balance models. J Geophys Res 1985;90(D1):2191–205.

[53] Hoekstra AY. The water submodel: AQUA. In: Rotmans J, de Vries BJM, editors. Perspectives on global change: the TARGETS approach. Cambridge, UK: Cambridge University Press; 1997. p. 107–34.

[54] Huntington TG. Evidence for intensification of the global water cycle: review and synthesis. J Hydrol 2006;319(1–4):83–95.

[55] Hurd BH, Callaway M, Smith J, Kirshen P. Climatic change and US water resources: from modeled watershed impacts to national estimates. J Am Water Resour Assoc 2004;40(1):129–48.

[56] Iglesias E, Blanco M. New directions in water resources management: the role of water pricing policies. Water Resour Res 2008;44(W06417). doi:10.1029/2006WR005708.

[57] Jury WA, Vaux HJ. The emerging global water crisis: managing scarcity and conflict between water users. Adv Agron 2007;95:1–76.

[58] Kadoya T, Sasaki T, Ihara S, Larose E, Sanford M, Graham AK, et al. Utilizing system dynamics modeling to examine impact of deregulation on generation capacity growth. Proc IEEE 2005;93(11):2060–9.

[59] Keeling CD, Whorf TP. Atmospheric CO_2 records from sites in the SIO air sampling network. In: Trends: a compendium of data on global change. Oak Ridge, Tennessee: Carbon Dioxide Information Analysis Center, Oak Ridge National Laboratory, US Department of Energy; 2005.

[60] Kim SH, Edmonds J, Lurz J, Smith SJ, Wise M. The O^{bj}ECTS framework for integrated assessment: hybrid modeling of transportation. Energy J 2006:63–91 [special issue].

[61] Langsdale S, Beall A, Carmichael J, Cohen S, Forster C. An exploration of water resources futures under climate change using system dynamics modeling. Integr Assess 2007;7(1):51–79.

[62] Leal AD, Legey LFL, Gonzalez-Araya MC, Jablonski S. A system dynamics model for the environmental management of the Sepetiba Bay watershed, Brazil. Environ Manage 2006;38(5):879–88.

[63] Liu J, You L, Amini M, Obersteiner M, Herrero M, Zehnder AJB, et al. A high-resolution assessment on global nitrogen flows in cropland. Proc Natl Acad USA 2010;107(17):8035–40.

[64] Madani K, Mariño MA. System dynamics analysis for managing Iran's Zayandeh-Rud river basin. Water Resour Manage 2009;23(11):2163–87.

[65] Maddison A. The world economy: a millennial perspective. Paris: Organisation for Economic Co-operation and Development; 2001.

[66] Maddison A. The world economy: historical perspective. Paris: Organisation for Economic Co-operation and Development; 2003.

[67] Manabe S, Wetherald RT, Milly PCD, Delworth TL, Stouffer RJ. Century-scale change in water availability: CO_2-quadrupling experiment. Clim Change 2004;64(1–2):59–76.

[68] Marland G, Boden TA, Andres RJ. Global, regional, and national CO_2 emissions. In: Trends: a compendium of data on global change. Oak Ridge, Tennessee: Carbon Dioxide Information Analysis Center, US Department of Energy; 2007.

[69] Meadows DH, Randers J, Meadows D. Limits to growth: the thirty year update. White River Junction, Vermont: Chelsea Green Publishing Company; 2004.

[70] Monfreda C, Ramankutty N, Foley JA. Farming the planet: 2. Geographic distribution of crop areas, yields, physiological types, and net primary production in the year 2000. Global Biogeochem Cycles 2008;22(GB1022). doi:10.1029/2007GB002947.

[71] Nakicenovic N, Swart R. IPCC special report on emissions scenarios. Cambridge UK: Cambridge University Press; 2000.

[72] Netherlands Environmental Assessment Agency (MNP). Integrated modelling of global environmental change. An overview of IMAGE 2.4. Report no. 500110002/2006, Netherlands Environmental Assessment Agency (MNP), Bilthoven, The Netherlands; 2006.

[73] Nordhaus WD. A question of balance: weighing the options on global warming policies. New Haven, Connecticut: Yale University Press; 2008.

[74] Nordhaus WD, Boyer J. Warming the world: economic models of global warming. Cambridge, Massachusetts: The MIT Press; 2000.

[75] Paredes-Arquiola J, Andreu-Alvarez J, Martin-Monerris M, Solera A. Water quantity and quality models applied to the Jucar River basin, Spain. Water Resour Manage 2010;24(11):2759–79.

[76] Parson EA, Fisher-Vanden K. Integrated assessment models of global change. Annu Rev Energy Environ 1997;22:589–628.

[77] Postel SL. Water for food production: will there be enough in 2025? BioScience 1998;48(8):629–37.

[78] Postel S. Pillar of sand: can the irrigation miracle last? 1st ed. New York: W.W. Norton; 1999.

[79] Postel SL, Daily GC, Ehrlich PR. Human appropriation of renewable fresh water. Science 1996;271(5250):785–8.
[80] Prodanovic P, Simonovic SP. An operational model for support of integrated watershed management. Water Resour Manage 2010;24(6):1161–94.
[81] Richmond B. Systems thinking: critical thinking skills for the 1990s and beyond. Syst Dyn Rev 1993;9(2):113–33.
[82] Rijsberman FR. Water scarcity: fact or fiction? Agric Water Manage 2006;80(1–3):5–22.
[83] Rockström J, Falkenmark M, Karlberg L, Hoff H, Rost S, Gerten D. Future water availability for global food production: the potential of green water for increasing resilience to global change. Water Resour Res 2009;45(W00A12). doi:10.1029/2007WR006767.
[84] Rockström J, Gordon L. Assessment of green water flows to sustain major biomes of the world: implications for future ecohydrological landscape management. Phys Chem Earth B – Hydrol Ocean Atmos 2001;26(11–12):843–51.
[85] Rockström J, Lannerstad M, Falkenmark M. Assessing the water challenge of a new green revolution in developing countries. Proc Natl Acad Sci USA 2007;104(15):6253–60.
[86] Rost S, Gerten D, Bondeau A, Lucht W, Rohwer J, Schaphoff S. Agricultural green and blue water consumption and its influence on the global water system. Water Resour Res 2008;44(W09405). doi:10.1029/2007WR006331.
[87] Rotmans J, de Vries B. Perspectives on global change: the TARGETS approach. Cambridge, UK: Cambridge University Press; 1997.
[88] Rotmans J, van Asselt MBA, de Vries BJM. Global change and sustainable development. In: Rotmans J, de Vries B, editors. Perspectives on global change: the TARGETS approach. Cambridge, UK: Cambridge University Press; 1997. p. 1–14.
[89] Schlesinger WH. On the fate of anthropogenic nitrogen. Proc Natl Acad USA 2009;106(1):203–8.
[90] Shen YJ, Ok T, Utsumi N, Kanae S, Hanasaki N. Projection of future world water resources under SRES scenarios: water withdrawal. Hydrol Sci J 2008;53(1):11–33.
[91] Shiklomanov IA. Appraisal and assessment of world water resources. Water Int 2000;25(1):11–32.
[92] Siebert S, Döll P. Quantifying blue and green virtual water contents in global crop production as well as potential production losses without irrigation. J Hydrol 2010;384(3–4):198–217.
[93] Simonovic SP, Davies EGR. Are we modelling impacts of climatic change properly? Hydrol Process 2006;20(2):431–3.
[94] Simonovic SP. World water dynamics: global modeling of water resources. J Environ Manage 2002;66:249–67.
[95] Simonovic SP. Managing water resources: methods and tools for a systems approach. London: Earthscan Publications Ltd.; 2009.
[96] Sivapalan M, Bloschl G, Zhang L, Vertessy R. Downward approach to hydrological prediction. Hydrol Process 2003;17(11):2101–11.
[97] Sterman JD. Business dynamics: systems thinking and modeling for a complex world. Boston, Massachusetts: The McGraw-Hill Companies Ltd.; 2000.
[98] Sterman JD. Risk communication on climate: mental models and mass balance. Science 2008;322:532–3.
[99] Tanaka SK, Zhu TJ, Lund JR, Howitt RE, Jenkins MW, Pulido MA, et al. Climate warming and water management adaptation for California. Clim Change 2006;76(3–4):361–87.
[100] Teegavarapu RSV, Tangirala AK, Ormsbee L. Modeling water quality management alternatives for a nutrient impaired stream using system dynamics simulation. J Environ Inform 2005;5(2):73–81.
[101] The World Bank Group [Internet]. WDI online, DDP quick query. c2007 [cited 2007 April 18]. Available from: <http://ddp-ext.worldbank.org/ext/DDPQQ>.
[102] Tidwell VC, Passell HD, Conrad SH, Thomas RP. System dynamics modeling for community-based water planning: application to the Middle Rio Grande. Aquat Sci 2004;66(4):357–72.
[103] Tol RSJ. Integrated assessment modelling. Report no. FNU-102, Hamburg University and Centre for Marine and Atmospheric Science, Hamburg, Germany; 2006.
[104] United Nations Department of Economic and Social Affairs (UNESA) [Internet]. World population prospects: the 2006 revision population database; c2006 [cited 2006 November 12]. Available from: <http://esa.un.org/unpp>.
[105] Vassolo S, Döll P. Global-scale gridded estimates of thermoelectric power and manufacturing water use. Water Resour Res 2005;41(W04010). doi:10.1029/2004WR003360.
[106] Vinnikov KY, Grody NC, Robock A, Stouffer RJ, Jones PD, Goldberg MD. Temperature trends at the surface and in the troposphere. J Geophys Res – Atmos 2006;111(D03106). doi:10.1029/2005JD006392.
[107] Vivoni ER, Aragón CA, Malczynski L, Tidwell VC. Semiarid watershed response in central New Mexico and its sensitivity to climate variability and change. Hydrol Earth Syst Sci 2009;13:715–33.
[108] Vörösmarty CJ, Green P, Salisbury J, Lammers RB. Global water resources: vulnerability from climate change and population growth. Science 2000;289(5477):284–8.
[109] Wagener T, Sivapalan M, Troch PA, McGlynn BL, Harman CJ, Gupta HV, et al. The future of hydrology: an evolving science for a changing world. Water Resour Res 2010;46(W05301). doi:10.1029/2009WR008906.
[110] Williams A, Lansey K, Washburne J. A dynamic simulation based water resources education tool. J Environ Manage 2009;90(1):471–82.
[111] Wirsenius S. Efficiencies and biomass appropriation of food commodities on global and regional levels. Agric Syst 2003;77(3):219–55.
[112] Wise M, Calvin K, Thomson A, Clarke L, Bond-Lamberty B, Sands R, et al. Implications of limiting CO_2 concentrations for land use and energy. Science 2009;324(5931):1183–6.
[113] Wollheim WM, Vörösmarty CJ, Bouwman AF, Green P, Harrison J, Linder E, et al. Global N removal by freshwater aquatic systems using a spatially distributed, within-basin approach. Global Biogeochem Cycles 2008;22(GB2026). doi:10.1029/2007GB002963.
[114] Xu ZX, Takeuchi K, Ishidaira H, Zhang XW. Sustainability analysis for Yellow River water resources using the system dynamics approach. Water Resour Manage 2002;16(3):239–61.
[115] Zhang W, Wang Y, Peng H, Li Y, Tang J, Wu KB. A coupled water quantity–quality model for water allocation analysis. Water Resour Manage 2010;24(3):485–511.